

Multiple Testing of Local Extrema for Detection of Structural Breaks in Piecewise Linear Models

Zhibing He¹, Dan Cheng^{1,*} and Yunpeng Zhao²

¹Arizona State University, Tempe, AZ

²Colorado State University, Fort Collins, CO

*Corresponding author. Email: dcheng17@asu.edu

Abstract

In this paper, we propose a new generic method for detecting the number and locations of structural breaks or change points in piecewise linear models under stationary Gaussian noise. Our method transforms the change point detection problem into identifying local extrema (local maxima and local minima) through kernel smoothing and differentiation of the data sequence. By computing p-values for all local extrema based on peak height distributions of smooth Gaussian processes, we utilize the Benjamini-Hochberg procedure to identify significant local extrema as the detected change points. Our method can distinguish between two types of change points: continuous breaks (Type I) and jumps (Type II). We study three scenarios of piecewise linear signals, namely pure Type I, pure Type II and a mixture of Type I and Type II change points. The results demonstrate that our proposed method ensures asymptotic control of the False Discover Rate (FDR) and power consistency, as sequence length, slope changes, and jump size increase. Furthermore, compared to traditional change point detection methods based on recursive segmentation, our approach only requires a single test for all candidate local extrema, thereby achieving the smallest computational complexity proportionate to the data sequence length. Additionally, numerical studies illustrate that our method maintains FDR control and power consistency, even in non-asymptotic cases when the size of slope changes or jumps is not large. We have implemented our method in the R package “dSTEM” (available from <https://cran.r-project.org/web/packages/dSTEM>).

Key Words: structural breaks, change points, piecewise linear models, kernel smoothing, multiple testing, Gaussian processes, peak height distribution, FDR, power consistency.

1 Introduction

In this paper, we consider a canonical univariate statistical model:

$$y(t) = \mu(t) + z(t), \quad t \in \mathbb{R}, \quad (1)$$

where $z(t)$ is correlated stationary Gaussian noise and $\mu(t)$ is a piecewise linear signal of the form

$$\mu(t) = c_j + k_j t, \quad t \in (v_{j-1}, v_j],$$

where $c_j, k_j \in \mathbb{R}$, $j = 1, 2, \dots$ and $-\infty = v_0 < v_1 < v_2 < \dots$. Assume the structures of $\mu(t)$ are different at neighboring v_j , i.e., $(c_j, k_j) \neq (c_{j+1}, k_{j+1})$, resulting in a continuous break or jump at v_j (see figure 1). Such v_j is called a change point or structural break.

The detection of structural breaks or change points plays a pivotal role in various fields, including statistics, econometrics, genomics, climatology and medical imaging. These detection methods are broadly applied to different domains based on different types of signals. For instance, in medical condition monitoring (Khan et al., 2020; Hann et al., 2009; Bulut et al., 2005) and image analysis (Liao and Pawlak, 1996; Kharinov, 2014), the presence of piecewise constant signals with jumps can indicate significant changes in patients' health conditions or object characteristics in images. Accurate detection of these changes is paramount for aiding in diagnosis, treatment planning, and object recognition tasks. On the other hand, piecewise linear signals with continuous breaks are commonly encountered in climate change research (Tomé and Miranda, 2004; Tebaldi and Lobell, 2008) and human activity analysis (Van Laerhoven et al., 2009; Lu et al., 2019). These changes may represent gradual shifts in temperature patterns or human behavior. Additionally, in financial markets, piecewise linear signals with noncontinuous breaks may indicate sudden shifts in stock prices or market dynamics (Chang et al., 2008; Ding et al., 2010). Monitoring and detecting these changes are crucial for making informed investment decisions and predicting market trends.

To differentiate between various ways of linear structure changes, we define the following two types of change points:

Definition 1. A point v_j is called a Type I change point (structural break) if $c_j + k_j v_j = c_{j+1} + k_{j+1} v_j$ and $k_j \neq k_{j+1}$, and a point v_j is denoted as a Type II change point if $c_j + k_j v_j \neq c_{j+1} + k_{j+1} v_j$ for $j \geq 1$.

At Type I change points v_j , the signals remain continuous, but the slopes experience a sudden change at v_j . Type II change points correspond to jumps in the signal, where there is a discontinuity between adjacent segments. Note that, a special case of Type II change points is that $\mu(t)$ is piecewise constant, i.e., $k_j \equiv 0$ and $c_j \neq c_{j+1}$ for $j \geq 1$. In this paper, we specifically focus on three scenarios of the signal $\mu(t)$, each representing different characteristics of change points. The scenarios are described as follows:

Scenario 1: Pure Type I Change Points. The signal $\mu(t)$ consists of continuous segments with slope changes at specific points v_j . Figure 1 (a) illustrates this scenario, where the signal exhibits continuous behavior with distinct slopes at the change points.

Scenario 2: Pure Type II Change Points. The signal $\mu(t)$ contains only Type II change points (jumps). Figure 1 (d) illustrates this scenario, where the signal exhibits sudden changes or discontinuities at change points.

Scenario 3: Mixture of Type I and Type II Change Points. The signal $\mu(t)$ combines both continuous breaks (Type I) and jumps (Type II) Figure 1 (g) illustrates this scenario, where it allows for a more general and realistic representation of signals with mixed characteristics.

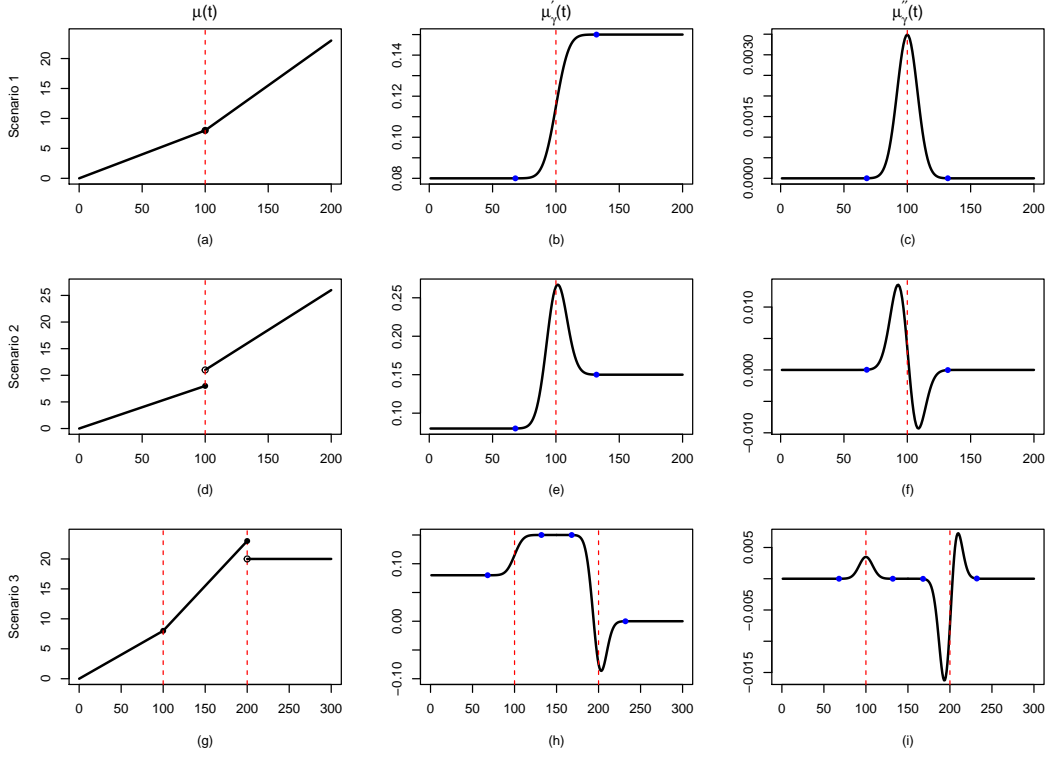


Figure 1: Illustration of change point detection. A change point in the piecewise linear signal $\mu(t)$ (left panel) becomes a local extremum in either the first derivative of the smoothed signal $\mu'_\gamma(t)$ (middle panel) or in the second derivative of the smoothed signal $\mu''_\gamma(t)$ (right panel). The red dashed lines indicate the locations of true change points, and the blue points represent the regions where the signal is smoothed using a Gaussian kernel. The top row shows a Type I change point v_j in $\mu(t)$ becomes a local extremum in $\mu''_\gamma(t)$ precisely at $t = v_j$. The middle row illustrates a Type II change point v_j in $\mu'_\gamma(t)$ becomes a local extremum in $\mu''_\gamma(t)$ around v_j . The bottom row shows that only Type II change points can generate local extrema in $\mu'_\gamma(t)$, whereas both Type I and Type II change points can generate local extrema in $\mu''_\gamma(t)$.

In this paper, our primary objective is to detect both the number of change points and their locations simultaneously. To address this problem, we propose a novel and generic approach that can handle an unknown number of multiple structural breaks occurring at unknown positions within the signal. Our proposed method for change point detection is illustrated and evaluated in three aforementioned scenarios (pure Type I change points, pure Type II change points, and a mixture of Type I and

Type II change points). Figure 1 shows the application of our method to each scenario, showcasing the mechanism behind our change point detection method.

The key idea behind our approach is based on the observation that a change point in the signal $\mu(t)$ will manifest as a local extremum (local maximum or local minimum) in either the first or second derivative of the smoothed signal. By kernel smoothing and differentiating the data sequence, we transform the problem of change point detection into identifying local extrema. Specifically,

- (i) A Type I change point in $\mu(t)$ becomes a local extremum in the second derivative $\mu''_\gamma(t)$ (see Figure 1 (a) and (c)).
- (ii) A Type II change point in $\mu(t)$ becomes a local extremum in the first derivative $\mu'_\gamma(t)$ (see Figure 1 (d) and (e)).

Therefore, in Scenario 1 and Scenario 2, the detection of change points relies on identifying local extrema in the second and the first derivatives of the smoothed signal respectively. However, in Scenario 3 a different approach is required due to the unique characteristics of each type:

- Type I change points do not generate local extrema in the first derivative $\mu'_\gamma(t)$ (see Figure 1 (b)). Therefore, in Scenario 3, the detection process begins by identifying all Type II change points as local extrema in $\mu'_\gamma(t)$.
- On the other hand, local extrema in the second derivative $\mu''_\gamma(t)$ can be generated by both Type I and Type II change points (see Figure 1 (i)). To detect Type I change points in Scenario 3, one needs to remove the local extrema in $\mu''_\gamma(t)$ generated by Type II change points.

By combining these approaches, our proposed method can distinguish between Type I and Type II change points in Scenario 3.

The detection of local extrema can be formulated as a peak detection problem, focusing on the local extrema of the first and second derivatives. In the literature, there have been notable contributions addressing this issue. One such notable approach is the Smoothing and TEsting of Maxima (STEM) algorithm (Schwartzman et al., 2011; Cheng and Schwartzman, 2017). The STEM algorithm aims to identify local maxima of the derivative as candidate peaks, which correspond to potential change points in the signal. By kernel smoothing the signal and applying multiple testing, the algorithm distinguishes between local extrema generated by true change points and those arising from random noise. Moreover, Cheng et al. (2020) introduced the differential STEM (dSTEM) method specifically designed for detecting change points in data sequences modeled as a piecewise constant signal-plus-noise. The dSTEM method leverages the principles of the STEM algorithm but adapts it to the piecewise constant signal model. This modification allows for more effective change point detection in scenarios where the signal exhibits piecewise constant behavior.

Literature on change point detection contains a vast amount of research work of statistical inference, but most of it specially designed for the case of a single change point with unknown location.

For example, for the case of a single change point with an unknown location, [Andrews \(1993\)](#) and [Andrews et al. \(1996\)](#) proposed comprehensive treatments and testing methods for structural change. [Perron \(1989\)](#) utilized unit root tests for detecting a one-time change in the level or slope of the trend function in univariate time series. [Bai \(1994\)](#) introduced the method of least squares for estimating an unknown shift point (change point) in a piecewise constant model. In recent years, there has been extensive interest in multiple change point detection, particularly in the context of multiple testing-based methods. In the piecewise constant signal model, [Yao and Au \(1989\)](#) studied least squares estimators for the locations and levels of the step function under both known and unknown numbers of jumps. [Lavielle \(2005\)](#) developed a penalized least squares method for estimating the number of change points and their locations. Binary segmentation (BS) ([Vostrikova, 1981](#)) is another popular approach, and [Hyun et al. \(2021\)](#) outlined similar post-selection tests for change point detection using Wild Binary Segmentation (WSB) ([Fryzlewicz, 2014](#)) and circular Binary Segmentation (CBS) ([Olshen et al., 2004](#)). SMUCE ([Frick et al., 2014](#); [Pein et al., 2017](#)) estimates the number of change points as the minimum among all candidate fits, where the empirical residuals pass a certain multi-scale test at a given significance level. [Li et al. \(2016\)](#) proposed an estimator that controls the False Discovery Rate (FDR) while allowing for a generous definition of a true discovery. FDR control was also demonstrated for the SaRa estimator ([Hao et al., 2013](#)) and the dSTEM estimator ([Cheng et al., 2020](#)) for multiple change point locations. For general piecewise linear signal models, [Bai and Perron \(1998\)](#) provided asymptotic distribution results regarding the distance between estimated change points and their true locations, assuming a known number of change points and a minimum distance of $O(L)$. However, the distributional limits depend on the unknown magnitudes of parameter changes, which can be challenging to estimate accurately. Additionally, methods such as narrowest-over-threshold (NOT) ([Baranowski et al., 2019](#)) and narrowest significance pursuit (NSP) ([Fryzlewicz, 2023](#)) have been proposed to detect change points by focusing on localized regions that contain suspected features. These works represent a diverse range of approaches for change point detection, providing valuable insights and methodologies for addressing both single and multiple change point scenarios in various signal models.

In this paper, we propose a modified Smoothing and TEsting of Maxima (mSTEM) algorithm for the change point detection in piecewise linear models under stationary Gaussian noise. Our proposed approach is unique in comparison with the existing literature in following ways:

1. Simultaneous estimation of the number and locations of change points. Our method allows for the estimation of both the number and locations of change points in the data simultaneously. By identifying significant local extrema in the first or second derivative under a global significance level, we provide a new framework for change point detection.
2. Differentiation between Type I and Type II change points. Our method can effectively distinguish between Type I and Type II change points. This capability is particularly useful in practical scenarios where researchers might be specifically interested in detecting jumps (Type

II) or continuous breaks (Type I).

3. Low computational complexity. Our proposed method achieves a significantly lower computational complexity compared to traditional change point detection methods. By testing only the candidate peaks generated by true change points or random noise once, the method reduces the computation to the number of candidate peaks, which proportionate to the length of data sequence L . Thus our proposed method can achieve lowest computational complexity of $O(L)$. This is a significant advantage, as most existing methods typically have computational costs of $O(L^2)$. The binary segmentation (BS) based method can achieve a lower computational complexity of order $O(L \log L)$ (Fryzlewicz, 2014).
4. General form of peak height distribution. A general and straightforward form of the peak height distribution in Gaussian Process. Unlike the results in Schwartzman et al. (2011); Cheng and Schwartzman (2017), the derived distribution depends on only one parameter.
5. Consideration of correlated noise. Our method takes into account the presence of correlated noise by assuming that the noise follows a Gaussian process. This is an important contribution, as many real-world datasets exhibit correlated noise (Hung et al., 2013), and our approach expands the applicability of change point detection methods to such scenarios.

This paper is organised as follows. Section 2 introduces the framework of our change point detection method. Section 3 provides change point detection algorithms under different scenarios and their asymptotic theories. Section 4 provides the simulation studies for various signal settings. Two real data studies are described in Section 5. Section 6 concludes with a brief discussion.

2 The mSTEM detection framework

2.1 The kernel smoothed signal

Consider the model (1). The jump size a_j at v_j is defined as

$$a_j = c_{j+1} + k_{j+1}v_j - (c_j + k_jv_j) = (c_{j+1} - c_j) + (k_{j+1} - k_j)v_j, j \geq 1. \quad (2)$$

By definition 1 a change point v_j is a Type I change point if $a_j = 0$ and a Type II change point if $a_j \neq 0$. Assume $d = \inf_j (v_j - v_{j-1}) > 0$ such that there is a minimal distance d between neighboring change points. In addition, we assume $k = \inf_j |k_{j+1} - k_j| > 0$ at Type I change points and $a = \inf_j |a_j| > 0$ at Type II change points respectively such that the slope changes and jump sizes do not become arbitrarily small.

Denote by $\phi(x)$ and $\Phi(x)$ the pdf and cdf of the standard normal distribution, respectively. Let $w_\gamma(t)$ be the Gaussian kernel with compact support $[-c\gamma, c\gamma]$ (we set $c = 4$ throughout the paper) and bandwidth γ , i.e.,

$$w_\gamma(t) = \frac{1}{\gamma} \phi\left(\frac{t}{\gamma}\right) \mathbb{1}\{-c\gamma \leq t \leq c\gamma\}. \quad (3)$$

Convolving the signal-plus-noise process (1) with the kernel $w_\gamma(t)$ leads to the generation of a smoothed random process:

$$y_\gamma(t) = w_\gamma(t) * y(t) = \int_{\mathbb{R}} w_\gamma(t-s)y(s) ds = \mu_\gamma(t) + z_\gamma(t), \quad (4)$$

where the smoothed signal and smoothed noise are defined respectively as

$$\mu_\gamma(t) = w_\gamma(t) * \mu(t) \quad \text{and} \quad z_\gamma(t) = w_\gamma(t) * z(t).$$

The smoothed noise $z_\gamma(t)$ is assumed to be a zero-mean and four-times differentiable stationary ergodic Gaussian process. To avoid the overlap of smoothing two neighboring change points, we assume that $d = \inf_j (v_j - v_{j-1})$ is large enough, say greater than $2c\gamma$.

2.2 Local extrema for derivatives of the smoothed signal

For a smooth function $f(t)$, denote by $f^{(\ell)}(t)$ its ℓ -th derivative, $\ell \geq 1$, and write by default $f'(t) = f^{(1)}(t)$ and $f''(t) = f^{(2)}(t)$ respectively. We have the following derivatives of the smoothed observed process (4),

$$y_\gamma^{(\ell)}(t) = w_\gamma^{(\ell)}(t) * y(t) = \int_{\mathbb{R}} w_\gamma^{(\ell)}(t-s)y(s) ds = \mu_\gamma^{(\ell)}(t) + z_\gamma^{(\ell)}(t), \quad (5)$$

where the derivatives of the smoothed signal and smoothed noise are respectively

$$\mu_\gamma^{(\ell)}(t) = w_\gamma^{(\ell)}(t) * \mu(t) \quad \text{and} \quad z_\gamma^{(\ell)}(t) = w_\gamma^{(\ell)}(t) * z(t), \quad \ell \geq 1.$$

The following lemmas on the first and second derivatives of the smoothed signal $\mu_\gamma(t)$ are useful in characterizing the extrema (see Figure 1). The proofs are provided in the Appendix.

Lemma 1. *The first and second derivatives of $\mu_\gamma(t)$ over $(v_{j-1} + c\gamma, v_{j+1} - c\gamma)$ are given respectively by*

$$\mu_\gamma'(t) = \begin{cases} k_j[2\Phi(c) - 1], & t \in (v_{j-1} + c\gamma, v_j - c\gamma), \\ \frac{a_j}{\gamma} \phi\left(\frac{v_j - t}{\gamma}\right) + (k_j - k_{j+1})\Phi\left(\frac{v_j - t}{\gamma}\right) + (k_j + k_{j+1})\Phi(c) - k_j, & t \in (v_j - c\gamma, v_j + c\gamma), \\ k_{j+1}[2\Phi(c) - 1], & t \in (v_j + c\gamma, v_{j+1} - c\gamma); \end{cases}$$

$$\mu_\gamma''(t) = \begin{cases} \frac{a_j(v_j - t) + (k_{j+1} - k_j)\gamma^2}{\gamma^3} \phi\left(\frac{v_j - t}{\gamma}\right), & t \in (v_j - c\gamma, v_j + c\gamma), \\ 0, & \text{otherwise,} \end{cases}$$

where a_j is the jump size defined by (2).

Lemma 2. *The local extremum of $\mu_\gamma'(t)$ over $(v_j - c\gamma, v_j + c\gamma)$ is achieved at*

$$t = \begin{cases} v_j + \gamma^2 q_j, & \text{if } a_j \neq 0, \\ \text{does not exist,} & \text{if } a_j = 0; \end{cases} \quad (6a)$$

$$(6b)$$

while the local extremum of $\mu''_\gamma(t)$ over $(v_j - c\gamma, v_j + c\gamma)$ is achieved at

$$t = \begin{cases} v_j + \frac{1}{2} \left(\gamma^2 q_j \pm \gamma \sqrt{\gamma^2 q_j^2 + 4} \right), & \text{if } a_j \neq 0, \\ v_j, & \text{if } a_j = 0, \end{cases} \quad (7a)$$

where $q_j = \frac{k_{j+1} - k_j}{a_j}$ for $a_j \neq 0$.

Recall that a_j is the size of jump at the change point v_j , thus v_j is a Type I change point if $a_j = 0$ and a Type II change point if $a_j \neq 0$. Note that q_j is the ratio between the change of slope and size of jump, and will be assumed to be small. It is seen that Lemma 2 characterizes the relation between the peak location of the differentiated smoothed signal and the original location v_j , yielding the following result.

Proposition 1. *A Type I change point v_j becomes a local extremum in $\mu''_\gamma(t)$ precisely at v_j (see (7b)); while a Type II change point v_j results in a local extremum in $\mu'_\gamma(t)$ at $v_j + \gamma^2 q_j$ (see (6a)), which tends to v_j as $q_j \rightarrow 0$.*

More specifically, as it can be seen from the proof that, a Type I change point v_j becomes a local maximum in $\mu''_\gamma(t)$ if $k_{j+1} - k_j > 0$ (a local minimum if $k_{j+1} - k_j < 0$); and a Type II change point v_j results in a local maximum in $\mu'_\gamma(t)$ near v_j if $a_j > 0$ (a local minimum if $a_j < 0$), regardless of the sign of $k_{j+1} - k_j$. Basically, Proposition 1 shows that the change points would be transformed to peaks in $\mu'_\gamma(t)$ or $\mu''_\gamma(t)$, providing the main idea on the detection in the pure cases Scenarios 1 and 2.

Remark 1. *Based on the results in Lemma 2, here we discuss the idea on detecting separately Types I and II change points in Scenario 3 where both types of change points exist. This will be shown in more details in Algorithm 3 below.*

First, note that a Type I change point does not generate any local extremum in $\mu'_\gamma(t)$ (see (6b)). This property is crucial to detect Type II change points via detecting peaks in $\mu'_\gamma(t)$ by Proposition 1 (see Step 1 in Algorithm 3). On the other hand, by (7a), a Type II change point v_j will generate a pair of local maximum and minimum in $\mu''_\gamma(t)$, with locations tending to $v_j \pm \gamma$ when q_j is sufficiently small. This will help us remove those local extrema in $\mu''_\gamma(t)$ generated from the detected Type II change points in the previous step and hence to detect the Type I change points via detecting peaks in $\mu'_\gamma(t)$ by Proposition 1 (see Step 2 in Algorithm 3).

Remark 2. *A Type II change point v_j with large $|q_j|$ behaves similarly to a Type I change point, its derivatives exhibit similar characteristics (see Figure 2 below). Specifically, a Type II change point with q_j large enough such that $q_j > c/\gamma$ can not generate a local extremum in the first derivative $\mu'_\gamma(t)$; and the corresponding second derivative $\mu''_\gamma(t)$ has only one local extremum around the change point v_j . Since $a_j \neq 0$ and $q_j > c/\gamma$, one has $v_j + \gamma^2 q_j > v_j + c\gamma$, implying no local extremum in the first derivative $\mu'_\gamma(t)$ (see (6a)). Additionally,*

$$v_j + \frac{1}{2} \left(\gamma^2 q_j + \gamma \sqrt{\gamma^2 q_j^2 + 4} \right) > v_j + c\gamma, \quad v_j + \frac{1}{2} \left(\gamma^2 q_j - \gamma \sqrt{\gamma^2 q_j^2 + 4} \right) \approx v_j. \quad (8)$$

Hence there is only one local extremum around v_j in the second derivative $\mu''_\gamma(t)$ (see (7a)). Given this behavior, it is reasonable to interpret a Type II change point with large $|q_j|$ as a special case that essentially behaves like Type I change points ($q_j = \infty$ as $a_j = 0$).

Intuitively, for a Type II change point v_j , if the $|q_j|$ is large enough such that $q_j > c/\gamma$, it means the slope change dominates the jump size, thereafter this Type II change point behaves similarly to a Type I change point. In this paper, we do not consider the case of large $|q_j|$. However, as discussed above, this case can be essentially treated as the case of Type I change points.

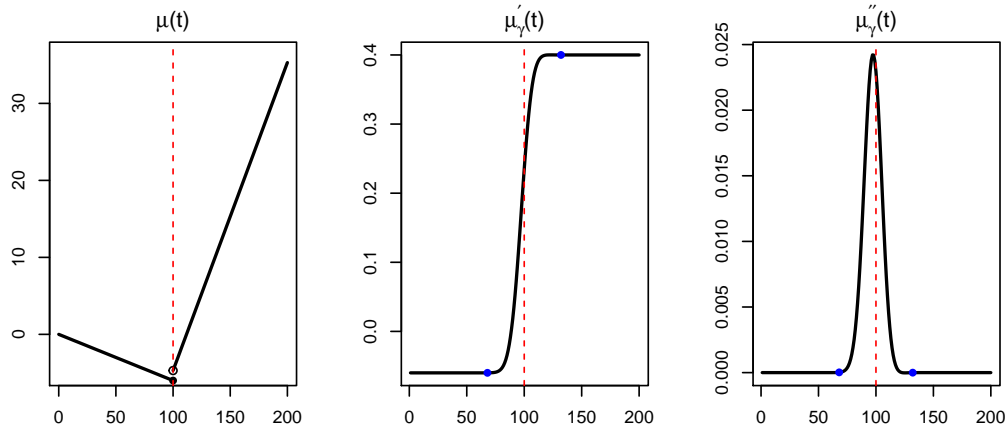


Figure 2: Characteristics of the Type II change point v_j with large $|q_j|$. In the left plot of signal $\mu(t)$, the slope change dominates the jump size, giving a large $|q_j|$. The middle plot of the first derivative μ'_γ shows no local extremum, and the right plot of the second derivative $\mu''_\gamma(t)$ shows a local maximum around the change point v_j . This special Type II change point can be essentially treated as a Type I change point.

2.3 Main ideas

Figure 1 demonstrates the key concept of our change point detection method. The main idea is to transform the problem of change point detection in a data sequence into a problem of testing local extrema either in the first or second derivative of the smoothed signal. A candidate peak can arise from either a true change points in the signal or random noise. Multiple testing based on the peak height distribution of the first and second derivatives is then employed to identify the significant peaks as the true change points. Notice that, although this main idea (or Figure 1) is illustrated over signal $\mu(t)$, it is also applicable to the signal-plus-noise $y(t)$ under certain asymptotic conditions such that the signal strength (size of jump or slope change) and length of data sequence are large; see conditions (C1) and (C2) below.

To further illustrate the main ideas of our method, toy examples are presented in Figure 3 and

Figure 4. In Scenario 1 (pure Type I change points), a Type I change point generates a peak exactly at its location in the second derivative $\mu''_\gamma(t)$, as indicated in (7b). In Scenario 2 (pure Type II change points), a Type II change point produces a peak in the first derivative $\mu'_\gamma(t)$ around its location, as described in (6a). By subtracting the corresponding baseline (piecewise slope at v_j) from the peaks in $y'_\gamma(t)$, the problem reduces to a standard peak detection problem. In Scenario 3, a combination of Type I and Type II change points is considered. The Type II change points are first identified based on the peaks in $y'_\gamma(t)$, and then the Type I change points are detected as significant peaks in $y''_\gamma(t)$ after cutting off the Type II change points.

Our proposed method, called mSTEM (**m**odified **S**oothing and **T**esting of **M**axima/**M**inima), consists of the following steps and provides a framework for change point detection.

1. Differential kernel smoothing: to transform change points into local maxima or minima (illustrated in Figure 1), and can meanwhile increase the signal-noise-ratio (SNR).
2. Candidate peaks: to find local extrumum of either the first or second derivative of the smoothed Gaussian process.
3. P-values: to compute the p-value of each local maximum or minimum under the null hypothesis of no signals in a local neighborhood.
4. Multiple testing: to apply a multiple testing procedure (Benjamini-Hochberg procedure) to the set of local maxima and minima, a change point is claimed to be detected if the p-value is significant.

3 Multiple change point detection for linear models

Suppose we observed $y(t)$ defined by (1) with J change points in the line of length L centered at the origin, which is denoted by $U(L) = (-L/2, L/2)$. We define the *signal region* as $\mathbb{S}_1 = \cup_{j=1}^J S_j = \cup_{j=1}^J (v_j - b, v_j + b)$, which is the region of interest where the true change points are expected to occur. It is defined as the union of intervals centered around each true change point v_j . The *null region* is the complement of the *signal region* within $U(L)$. It is given by $\mathbb{S}_0 = U(L) \setminus \mathbb{S}_1$, where no true change points are expected to occur.

3.1 Pure Type I change point detection

We consider the case of pure Type I change points, which do not generate any peak in $\mu'_\gamma(t)$ by (6b). Applying Proposition 1, it is appropriate to detect the Type I change points via detecting peaks in $y''_\gamma(t)$. Following the proposed mSTEM procedure of change point detection in Section 2.3, we give below the mSTEM algorithm for detection of the Type I change points.

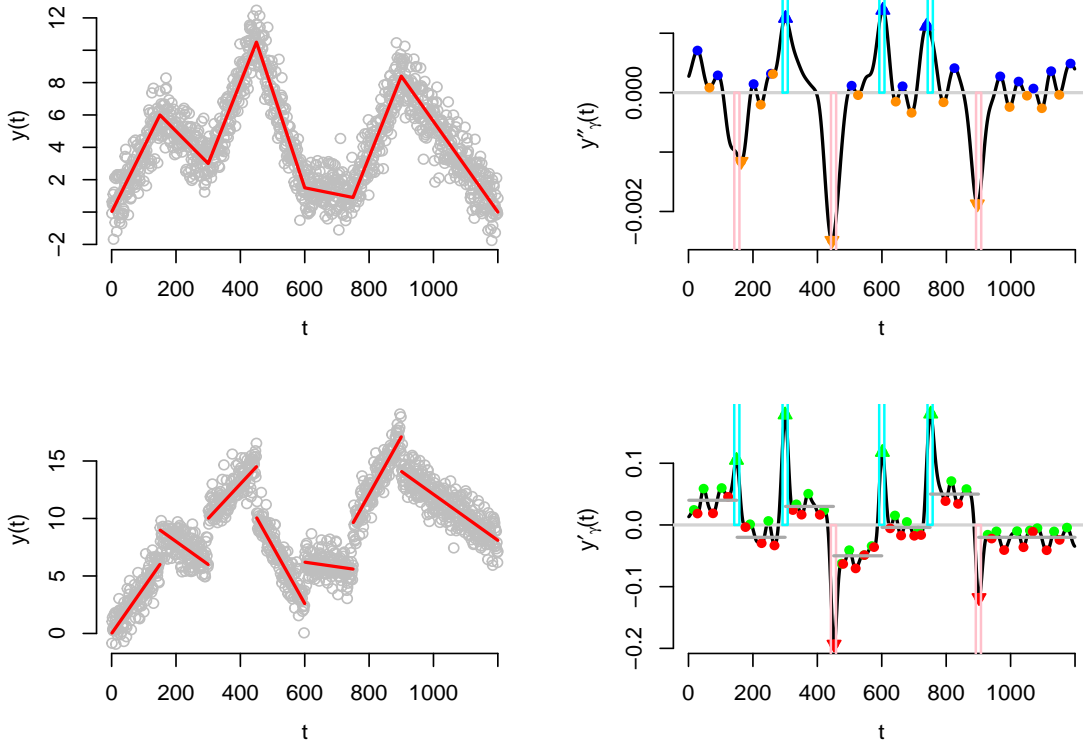


Figure 3: Process of Type I and Type II change point detection. The two plots on the left panel show the data (grey circles) with six Type I change points and the data with six Type II change points respectively. Here, the red lines indicate piecewise linear signals $\mu(t)$. The two plots (black lines) on the right panels show the second and first derivatives of the smoothed data respectively obtained from convolving data with the Gaussian kernel with bandwidth $\gamma = 8$. In the first derivative $y'_\gamma(t)$, local maxima and local minima are represented by green and red dots respectively. In the second derivative $y''_\gamma(t)$, they are represented by blue and orange dots respectively. The triangles indicate the significant local extrema under significant level $\alpha = 0.05$. The cyan and pink bars show the location tolerance intervals $(v_j - b, v_j + b)$ with $b = 5$ for the true increasing and decreasing change points respectively. The grey horizontal lines (lower right plot) indicate piecewise slopes of the signal, serving as baselines in the testing of $y'_\gamma(t)$. In these two testings, all change points of both Type I and Type II are detected perfectly without false discoveries.

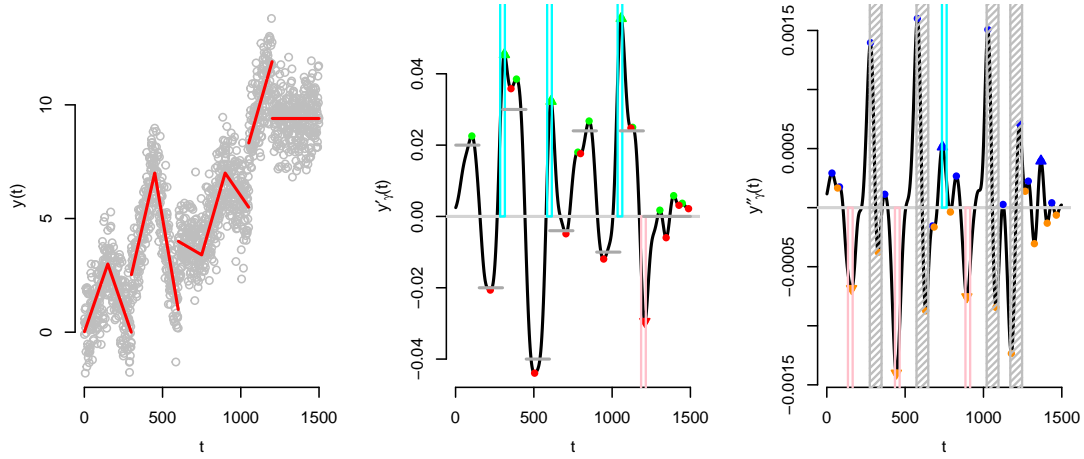


Figure 4: Process of mixture of Type I and Type II change point detection. The same graphical symbols and colors as in Figure 3 are utilized here. The left plot (grey circles) shows the data with four Type I and four Type II change points. The middle plot shows the first derivative of the smoothed data $y'_\gamma(t)$ for detection of Type II change points. The right plot shows the second derivative of the smoothed data $y''_\gamma(t)$. The Type II change points are detected first in the first derivative $y'_\gamma(t)$ (the middle plot). Then the local extrema in the second derivative $y''_\gamma(t)$ generated by the detected Type II change points are removed (represented by grey shaded bars and each bar is $[v_j - 2\gamma, v_j + 2\gamma]$). After this filtering process, the remaining significant local extrema in $y''_\gamma(t)$ are identified as Type I change points. In this testing, all the change points of both Type I and Type II are detected without false discoveries.

Algorithm 1 (mSTEM algorithm for Type I change point detection).

1. Differential kernel smoothing: Obtain the process $y''_\gamma(t)$ in (5) by convolution of $y(t)$ with the kernel derivative $w''_\gamma(t)$.
2. Candidate peaks: Find the set of local maxima and minima of $y''_\gamma(t)$ in $U(L)$, denoted by $\tilde{T}_1 = \tilde{T}_1^+ \cup \tilde{T}_1^-$, where

$$\begin{aligned}\tilde{T}_1^+ &= \left\{ t \in U(L) : y''_\gamma(t) = 0, y'''_\gamma(t) < 0 \right\}, \\ \tilde{T}_1^- &= \left\{ t \in U(L) : y''_\gamma(t) = 0, y'''_\gamma(t) > 0 \right\}.\end{aligned}$$

Note that \tilde{T}_1^+ is the set of local maxima in $y''_\gamma(t)$ and \tilde{T}_1^- represents the set of local minima.

3. P-values: For each $t \in \tilde{T}_1^+$, compute the p-value $p_1(t)$ for testing the hypotheses

$$\begin{aligned}\mathcal{H}_0(t) &: \{\mu_\gamma^{(3)}(s) = 0 \text{ for all } s \in (t-b, t+b)\} \text{ vs.} \\ \mathcal{H}_A(t) &: \{\mu_\gamma^{(3)}(s) > 0 \text{ for some } s \in (t-b, t+b)\};\end{aligned}$$

and for each $t \in \tilde{T}_1^-$, compute the p-value $p_1(t)$ for testing the hypotheses

$$\begin{aligned}\mathcal{H}_0(t) &: \{\mu_\gamma^{(3)}(s) = 0 \text{ for all } s \in (t-b, t+b)\} \text{ vs.} \\ \mathcal{H}_A(t) &: \{\mu_\gamma^{(3)}(s) < 0 \text{ for some } s \in (t-b, t+b)\},\end{aligned}$$

where $b > 0$ is an appropriate location tolerance parameter.

4. Multiple testing: Apply the Benjamini-Hochberg (BH) multiple testing procedure on the set of p-values $\{p_1(t), t \in \tilde{T}_1\}$, defined in Section 3.1.1 below, and declare all significant local extrema whose p-values are smaller than the significance threshold.

3.1.1 P-value calculation

The p-values in step 3 of Algorithm 1 is given by

$$p_1(t) = \begin{cases} F_{z''_\gamma}(y''_\gamma(t)) & t \in \tilde{T}_1^+, \\ F_{z''_\gamma}(-y''_\gamma(t)) & t \in \tilde{T}_1^-, \end{cases} \quad (9)$$

where $F_{z''_\gamma}(u)$ (defined in Section 3.4 below) is the right tail probability of $z''_\gamma(t)$ at the local maximum $t \in \tilde{T}_1$, evaluated under the null model $\mu''_\gamma(s) = 0, \forall s \in (t-b, t+b)$, i.e.,

$$F_{z''_\gamma}(u) = P(z''_\gamma(t) > u \mid t \text{ is a local maximum of } z''_\gamma(t)). \quad (10)$$

The second line in (9) is obtained by the following symmetry property and the fact that z''_γ and $-z''_\gamma$ have the same distribution,

$$\begin{aligned}& P(z''_\gamma(t) < y''_\gamma(t) \mid t \text{ is a local minimum of } z''_\gamma(t)) \\ &= P(-z''_\gamma(t) > -y''_\gamma(t) \mid t \text{ is a local maximum of } -z''_\gamma(t)) \\ &= F_{-z''_\gamma}(-y''_\gamma(t)) = F_{z''_\gamma}(-y''_\gamma(t)).\end{aligned}$$

3.1.2 Error and power definitions

For $u > 0$, we define $\tilde{T}_1(u) = \tilde{T}_1^+(u) \cup \tilde{T}_1^-(u)$, where

$$\begin{aligned}\tilde{T}_1^+(u) &= \left\{ t \in U(L) : y_\gamma''(t) > u, y_\gamma^{(3)}(t) = 0, y_\gamma^{(4)}(t) < 0 \right\}, \\ \tilde{T}_1^-(u) &= \left\{ t \in U(L) : y_\gamma''(t) < -u, y_\gamma^{(3)}(t) = 0, y_\gamma^{(4)}(t) > 0 \right\}.\end{aligned}$$

The above equations indicate that $\tilde{T}_1^+(u)$ and $\tilde{T}_1^-(u)$ are respectively the set of local maxima of $y_\gamma''(t)$ above u and the set of local minima of $y_\gamma''(t)$ below $-u$. The number of totally and falsely detected change points at threshold u are defined respectively as

$$R_1(u) = \#\{t \in \tilde{T}_1(u)\}, \quad V_1(u) = \#\{t \in \tilde{T}_1(u) \cap \mathbb{S}_0\}. \quad (11)$$

Both are defined as zero if $\tilde{T}_1(u)$ is empty. The FDR at threshold u is defined as the expected proportion of falsely detected change points

$$\text{FDR}_1(u) = \mathbb{E} \left\{ \frac{V_1(u)}{R_1(u) \vee 1} \right\}. \quad (12)$$

Denote by \mathcal{I}_1^+ and \mathcal{I}_1^- the collections of indices j corresponding to increasing and decreasing (in slope change) Type I change points respectively. The power is defined as

$$\begin{aligned}\text{Power}_1(u) &= \frac{1}{J} \left[\sum_{j \in \mathcal{I}_1^+} P \left(\tilde{T}_1^+(u) \cap (v_j - b, v_j + b) \neq \emptyset \right) \right. \\ &\quad \left. + \sum_{j \in \mathcal{I}_1^-} P \left(\tilde{T}_1^-(u) \cap (v_j - b, v_j + b) \neq \emptyset \right) \right],\end{aligned} \quad (13)$$

where each $P(\cdot)$ is the probability of detecting change point v_j within a distance b . It is seen that this power is the average probability of detecting true change points v_j within a distance b .

3.1.3 Asymptotic FDR control and power consistency

Denote by $E[\tilde{m}_{z_\gamma''}(U(1))]$ and $E[\tilde{m}_{z_\gamma''}(U(1), u)]$ the expected number of local extrema, and the expected number of both local maxima above level u and local minima below $-u$ of $z_\gamma''(t)$ on the unit interval $U(1) = (-1/2, 1/2)$, respectively. Note that, by symmetry, the expected number of local minima of $z_\gamma''(t)$ below level $-u$ equals the expected number of local maxima of $z_\gamma''(t)$ above u , which is $E[\tilde{m}_{z_\gamma''}(U(1), u)]/2$. Similarly, we define accordingly $E[\tilde{m}_{z_\gamma'}(U(1))]$ and $E[\tilde{m}_{z_\gamma'}(U(1), u)]$ for $z_\gamma'(t)$ on $U(1)$.

Recall that the BH procedure applied in step 4 of Algorithm 1 is defined as follows. Let m_1 be the size of the set \tilde{T}_1 . For a fixed $\alpha \in (0, 1)$, let ℓ be the largest index for which the i th smallest p-value is less than $i\alpha/m_1$. Then the null hypothesis $\mathcal{H}_0(t)$ at $t \in \tilde{T}_1$ is rejected if

$$p_1(t) < \frac{\ell\alpha}{m_1} \iff \begin{cases} y_\gamma''(t) > \tilde{u}_1 = F_{z_\gamma''}^{-1} \left(\frac{\ell\alpha}{m_1} \right) & \text{if } t \in \tilde{T}_1^+, \\ y_\gamma''(t) < -\tilde{u}_1 = -F_{z_\gamma''}^{-1} \left(\frac{\ell\alpha}{m_1} \right) & \text{if } t \in \tilde{T}_1^-, \end{cases} \quad (14)$$

where $\ell\alpha/m_I$ is defined as 1 if $m_I = 0$. Note that \tilde{T}_I and hence m_I and \tilde{u}_I are also random, which are different from the usual BH procedure. We define FDR in such BH procedure as

$$\text{FDR}_{I,\text{BH}} = E \left\{ \frac{V_I(\tilde{u}_I)}{R_I(\tilde{u}_I) \vee 1} \right\}, \quad (15)$$

where $R_I(\cdot)$ and $V_I(\cdot)$ are defined in (11) and the expectation is taken over all possible realizations of the random threshold \tilde{u}_I . Similarly, the corresponding power, denoted by $\text{Power}_{I,\text{BH}}$, is defined as (13) with u replaced by \tilde{u}_I .

For the asymptotic theories of Type I change point detection, we make the assumption:

$$(C1) \quad L \rightarrow \infty, k = \inf_j |k_{j+1} - k_j| \rightarrow \infty, \text{ and } k^2 / \log L \rightarrow \infty.$$

Theorem 1. *Suppose that $y(t)$ contains only Type I change points, the condition (C1) holds and $J/L \rightarrow A > 0$ as $L \rightarrow \infty$.*

(i) *If Algorithm 1 is applied with a fixed threshold u , then*

$$\text{FDR}_I(u) \rightarrow \frac{E[\tilde{m}_{z''_\gamma}(U(1), u)](1 - 2c\gamma A)}{E[\tilde{m}_{z''_\gamma}(U(1), u)](1 - 2c\gamma A) + A}, \quad (16)$$

$$\text{Power}_I(u) \rightarrow 1. \quad (17)$$

(ii) *If Algorithm 1 is applied with random threshold \tilde{u}_I , then*

$$\text{FDR}_{I,\text{BH}} \rightarrow \alpha \frac{E[\tilde{m}_{z''_\gamma}(U(1))](1 - 2c\gamma A)}{E[\tilde{m}_{z''_\gamma}(U(1))](1 - 2c\gamma A) + A}, \quad (18)$$

$$\text{Power}_{I,\text{BH}} \rightarrow 1. \quad (19)$$

Note that, by the definition of d , we have $Jd < L$ or $d < J/L \rightarrow A$. Meanwhile, it is assumed $d = \inf_j (v_j - v_{j-1}) > 2c\gamma$, thus we always have $A > 2c\gamma$ and hence $1 - 2c\gamma A > 0$.

3.2 Pure Type II change point detection

In the detection of Type I breaks, the piecewise slopes of $\mu(t)$ will be 0 in $\mu''_\gamma(t)$ except in the smoothed *signal region*, denoted by $\mathbb{S}_{1,\gamma} = \cup_{j=1}^J (v_j - c\gamma, v_j + c\gamma)$ (see the intervals indicated by the blue points in Figure 1). However, in the detection of Type II breaks, the piecewise slopes become piecewise constants (not zeros) in $\mu'_\gamma(t)$ except in the smoothed *signal region*. To detect Type II breaks, the null hypothesis (no signal) $\mu'_\gamma(t) - k(t)$, where $k(t)$ are these piecewise constants, will be tested. Hence, it is crucial to estimate the piecewise slopes around the change points v_j .

3.2.1 Piecewise slopes estimate

The main idea of estimation of piecewise slopes is to divide the data sequence into segments and estimate the slopes within each segment using linear regression. These segments are determined based on the presence of pairwise local maxima and minima around change points ($v_j - \gamma$ and $v_j + \gamma$) in the second derivative $\mu''_\gamma(t)$ (see Figure 1 (f)).

To ensure that all true Type II breaks are captured and to give a better estimate of the piecewise slopes, Algorithm 1 is followed with a larger significance level, such as 0.1. This helps in obtaining non-conservative initial estimators for Type II change points based on the peaks detected in $y''_\gamma(t)$. Then within each segment the piecewise slope is estimated using a robust regression model (Huber, 2004) to mitigate the disturbance of change points.

Algorithm 2 (mSTEM algorithm for Type II change point detection).

1. Differential kernel smoothing: Obtain the process $y'_\gamma(t)$ in (5) by convolution of $y(t)$ with the kernel derivative $w'_\gamma(t)$.
2. Candidate peaks: Find the set of local maxima and minima of $y'_\gamma(t)$ in $U(L)$, denoted by $\tilde{T}_\Pi = \tilde{T}_\Pi^+ \cup \tilde{T}_\Pi^-$, where

$$\begin{aligned}\tilde{T}_\Pi^+ &= \left\{ t \in U(L) : y''_\gamma(t) = 0, y_\gamma^{(3)}(t) < 0 \right\}, \\ \tilde{T}_\Pi^- &= \left\{ t \in U(L) : y''_\gamma(t) = 0, y_\gamma^{(3)}(t) > 0 \right\}.\end{aligned}$$

3. P-values: For each $t \in \tilde{T}_\Pi^+$, compute the p-value $p_\Pi(t)$ for testing the hypotheses

$$\begin{aligned}\mathcal{H}_0(t) &: \{ \mu'_\gamma(s) - k(s) = 0 \text{ for all } s \in (t - b, t + b) \} \quad \text{vs.} \\ \mathcal{H}_A(t) &: \{ \mu'_\gamma(s) - k(s) > 0 \text{ for some } s \in (t - b, t + b) \},\end{aligned}$$

where $k(s)$ is the piecewise slope. For each $t \in \tilde{T}_\Pi^-$, compute the p-value $p_\Pi(t)$ for testing the hypotheses

$$\begin{aligned}\mathcal{H}_0(t) &: \{ \mu'_\gamma(s) - k(s) = 0 \text{ for all } s \in (t - b, t + b) \} \quad \text{vs.} \\ \mathcal{H}_A(t) &: \{ \mu'_\gamma(s) - k(s) < 0 \text{ for some } s \in (t - b, t + b) \},\end{aligned}$$

4. Multiple testing: Apply the BH multiple testing procedure on the set of p-values $\{p_\Pi(t), t \in \tilde{T}_\Pi\}$, and declare significant all local extrema whose p-values are smaller than the significance threshold.

3.2.2 Error and power definitions

For $u > 0$, we define $\tilde{T}_\Pi(u) = \tilde{T}_\Pi^+(u) \cup \tilde{T}_\Pi^-(u)$, where

$$\begin{aligned}\tilde{T}_\Pi^+(u) &= \left\{ t \in U(L) : y'_\gamma(t) - k(t) > u, y''_\gamma(t) = 0, y_\gamma^{(3)}(t) < 0 \right\}, \\ \tilde{T}_\Pi^-(u) &= \left\{ t \in U(L) : y'_\gamma(t) - k(t) < -u, y''_\gamma(t) = 0, y_\gamma^{(3)}(t) > 0 \right\}.\end{aligned}$$

The number of totally and falsely detected change points and the FDR at threshold u are defined respectively as

$$R_{\text{II}}(u) = \#\{t \in \tilde{T}_{\text{II}}(u)\}, \quad V_{\text{II}}(u) = \#\{t \in \tilde{T}_{\text{II}}(u) \cap \mathbb{S}_0\}, \quad \text{FDR}_{\text{II}}(u) = \mathbb{E} \left\{ \frac{V_{\text{II}}(u)}{R_{\text{II}}(u) \vee 1} \right\}. \quad (20)$$

Denote by $\mathcal{I}_{\text{II}}^+$ and $\mathcal{I}_{\text{II}}^-$ the collections of indices j corresponding to increasing and decreasing (in jump) Type II change points v_j , respectively. The power is defined as

$$\begin{aligned} \text{Power}_{\text{II}}(u) = \frac{1}{J} & \left[\sum_{j \in \mathcal{I}_{\text{II}}^+} P \left(\tilde{T}_{\text{II}}^+(u) \cap (v_j - b, v_j + b) \neq \emptyset \right) \right. \\ & \left. + \sum_{j \in \mathcal{I}_{\text{II}}^-} P \left(\tilde{T}_{\text{II}}^-(u) \cap (v_j - b, v_j + b) \neq \emptyset \right) \right]. \end{aligned} \quad (21)$$

3.2.3 Asymptotic FDR control and power consistency

Suppose the BH procedure is applied in step 4 of Algorithm 2 as follows. Define m_{II} as the size of set \tilde{T}_{II} . For a fixed $\alpha \in (0, 1)$, let ℓ be the largest index for which the i th smallest p-value is less than $i\alpha/m_{\text{II}}$. Then the null hypothesis $\mathcal{H}_0(t)$ at $t \in \tilde{T}_{\text{II}}$ is rejected if

$$p_{\text{II}}(t) < \frac{\ell\alpha}{m_{\text{II}}} \iff \begin{cases} y'_\gamma(t) - k(t) > \tilde{u}_{\text{II}} = F_{z'_\gamma}^{-1} \left(\frac{\ell\alpha}{m_{\text{II}}} \right) & \text{if } t \in \tilde{T}_{\text{II}}^+, \\ y'_\gamma(t) - k(t) < -\tilde{u}_{\text{II}} = -F_{z'_\gamma}^{-1} \left(\frac{\ell\alpha}{m_{\text{II}}} \right) & \text{if } t \in \tilde{T}_{\text{II}}^-, \end{cases} \quad (22)$$

where $\ell\alpha/m_{\text{II}}$ is defined as 1 if $m_{\text{II}} = 0$. Since \tilde{u}_{II} is random, we define FDR in such BH procedure as

$$\text{FDR}_{\text{II,BH}} = \mathbb{E} \left\{ \frac{V_{\text{II}}(\tilde{u}_{\text{II}})}{R_{\text{II}}(\tilde{u}_{\text{II}}) \vee 1} \right\},$$

where $R_{\text{II}}(\cdot)$ and $V_{\text{II}}(\cdot)$ are defined in (20) and the expectation is taken over all possible realizations of the random threshold \tilde{u}_{II} . Similarly, the corresponding power, denoted by $\text{Power}_{\text{II,BH}}$, is defined as (13) with u replaced by \tilde{u}_{II} .

For the asymptotic theories of Type II change point detection, we make the assumption:

$$(C2) \quad a = \inf_j |a_j| \rightarrow \infty, \quad q = \sup_j \left| \frac{k_{j+1} - k_j}{a_j} \right| \rightarrow 0 \quad \text{and} \quad \log L/a^2 \rightarrow 0 \quad \text{as } L \rightarrow \infty.$$

Theorem 2. *Suppose $y(t)$ contains only Type II change points, the condition (C2) holds and $J/L \rightarrow A > 0$ as $L \rightarrow \infty$.*

(i) *If Algorithm 2 is applied with a fixed threshold u , then*

$$\text{FDR}_{\text{II}}(u) \rightarrow \frac{E[\tilde{m}_{z'_\gamma}(U(1), u)](1 - 2c\gamma A)}{E[\tilde{m}_{z'_\gamma}(U(1), u)](1 - 2c\gamma A) + A}, \quad (23)$$

$$\text{Power}_{\text{II}}(u) \rightarrow 1. \quad (24)$$

(ii) If Algorithm 2 is applied with random threshold \tilde{u}_{II} , then

$$\text{FDR}_{\text{II,BH}} \rightarrow \alpha \frac{E[\tilde{m}_{z'_\gamma}(U(1))](1 - 2c\gamma A)}{E[\tilde{m}_{z'_\gamma}(U(1))](1 - 2c\gamma A) + A}, \quad (25)$$

$$\text{Power}_{\text{II,BH}} \rightarrow 1. \quad (26)$$

3.3 Mixture of Type I and Type II change point detection

Pure Type I change points can be detected through peak detection in the second derivative, $y''_\gamma(t)$ (see Algorithm 1), and pure Type II change points can be detected using peak detection in the first derivative, $y'_\gamma(t)$ (see Algorithm 2). However, it is very common that a real signal contains both Type I and Type II change points. Distinguishing between Type I and Type II change points is a key challenge when dealing with signals that contain a mixture of both types. Our approach is to first detect Type II change points through peak detection in the first derivative $y'_\gamma(t)$, and then detect Type I change points by excluding the locations of Type II change points from consideration in the second derivative $y''_\gamma(t)$. The reason is as follows:

1. Type II change points generate peaks in the first derivative $y'_\gamma(t)$, while Type I change points do not. By detecting significant peaks in $y'_\gamma(t)$ using Algorithm 2, we can identify the locations of Type II change points.
2. Once the Type II change points are identified, we can focus on detecting Type I change points. Both Type I and Type II change points generate peaks in the second derivative $y''_\gamma(t)$. However, some of these peaks may be generated by Type II change points, and we want to exclude them from our Type I detection.

To distinguish between Type I and Type II change points in the mixture case, we remove the Type II change points detected in the first step from consideration. This means that any peaks in the second derivative $y''_\gamma(t)$ that coincide with the locations of Type II change points are excluded from the set of potential Type I change points. The remaining peaks in $y''_\gamma(t)$, which are not associated with Type II change points, are more likely to be generated by Type I change points.

Algorithm 3 (mSTEM algorithm for mixture of Type I and II change point detection).

1. Detect Type II breaks: Perform Algorithm 2 to obtain estimates of Type II breaks, denoted as $\hat{v}_i \in \tilde{T}_{\text{II}}$ for $i = 1, 2, \dots$. A larger γ in this step is suggested to have a better estimate of Type II change points and less false discoveries. Because a larger γ generally results in a higher SNR (signal-to-noise ratio, see Section 3.5).
2. Candidate Type I peaks: Find the set of local maxima and minima of $y''_\gamma(t)$ in $U(L)$, denoted by $\tilde{T}_{\text{I}} = \tilde{T}_{\text{I}}^+ \cup \tilde{T}_{\text{I}}^-$. As \tilde{T}_{I} contains local extrema generated by both Type I and Type II breaks, it is necessary to remove the peaks generated by Type II breaks which are detected in step 1. Let

$\mathbb{S}_{\text{II}}^* = \cup_{i=1}(\hat{v}_i - 2\gamma, \hat{v}_i + 2\gamma)$ be the removed region, then the set of candidate peaks of Type I breaks is defined as $\tilde{T}_{\text{I}\backslash\text{II}} = \tilde{T}_{\text{I}\backslash\text{II}}^+ \cup \tilde{T}_{\text{I}\backslash\text{II}}^-$, where

$$\begin{aligned}\tilde{T}_{\text{I}\backslash\text{II}}^+ &= \tilde{T}_{\text{I}}^+ \setminus \mathbb{S}_{\text{II}}^*, \\ \tilde{T}_{\text{I}\backslash\text{II}}^- &= \tilde{T}_{\text{I}}^- \setminus \mathbb{S}_{\text{II}}^*.\end{aligned}$$

3. P-values: For each $t \in \tilde{T}_{\text{I}\backslash\text{II}}^+$, compute the p-value $p_{\text{I}\backslash\text{II}}(t)$ for testing the hypotheses

$$\begin{aligned}\mathcal{H}_0(t) &: \{\mu''_\gamma(s) = 0 \text{ for all } s \in (t - b, t + b)\} \text{ vs.} \\ \mathcal{H}_A(t) &: \{\mu''_\gamma(s) > 0 \text{ for some } s \in (t - b, t + b)\};\end{aligned}$$

and for each $t \in \tilde{T}_{\text{I}\backslash\text{II}}^-$, compute the p-value $p_{\text{I}\backslash\text{II}}(t)$ for testing the hypotheses

$$\begin{aligned}\mathcal{H}_0(t) &: \{\mu''_\gamma(s) = 0 \text{ for all } s \in (t - b, t + b)\} \text{ vs.} \\ \mathcal{H}_A(t) &: \{\mu''_\gamma(s) < 0 \text{ for some } s \in (t - b, t + b)\}.\end{aligned}$$

4. Multiple testing: Apply a multiple testing procedure on the set of p-values $\{p_{\text{I}\backslash\text{II}}(t), t \in \tilde{T}_{\text{I}\backslash\text{II}}\}$, and declare significant all local extrema whose p-values are smaller than the significance threshold.

3.3.1 Asymptotic FDR control and power consistency

Let $\mathbb{S}_{1,\text{I}\backslash\text{II}} = \cup_{j=1}^J(v_j - b, v_j + b) \setminus \mathbb{S}_{\text{II}}^*$ be the signal region of Type I change points, and $\mathbb{S}_{0,\text{I}\backslash\text{II}} = U(L) \setminus \mathbb{S}_{1,\text{I}\backslash\text{II}}$ be the null region of Type I change points. Then the number of totally and falsely detected Type I change points at threshold u are defined respectively as

$$R_{\text{I}\backslash\text{II}}(u) = \#\{t \in \tilde{T}_{\text{I}\backslash\text{II}}(u)\}, \quad V_{\text{I}\backslash\text{II}}(u) = \#\{t \in \tilde{T}_{\text{I}\backslash\text{II}}(u) \cap \mathbb{S}_{0,\text{I}\backslash\text{II}}\}. \quad (27)$$

Given fixed thresholds u_1 and u_2 for Type I and Type II change point detection respectively, FDR is defined as

$$\text{FDR}_{\text{III}}(u_1, u_2) = \mathbb{E} \left\{ \frac{V_{\text{I}\backslash\text{II}}(u_1) + V_{\text{II}}(u_2)}{[R_{\text{I}\backslash\text{II}}(u_1) + R_{\text{II}}(u_2)] \vee 1} \right\},$$

and the power is defined as

$$\begin{aligned}\text{Power}_{\text{III}}(u_1, u_2) &= \frac{1}{J} \left[\sum_{j \in \mathcal{I}_1^+} P\left(\tilde{T}_{\text{I}\backslash\text{II}}^+(u_1) \cap (v_j - b, v_j + b) \neq \emptyset\right) + \sum_{j \in \mathcal{I}_1^-} P\left(\tilde{T}_{\text{I}\backslash\text{II}}^-(u_1) \cap (v_j - b, v_j + b) \neq \emptyset\right) \right. \\ &\quad \left. + \sum_{j \in \mathcal{I}_{\text{II}}^+} P\left(\tilde{T}_{\text{II}}^+(u_2) \cap (v_j - b, v_j + b) \neq \emptyset\right) + \sum_{j \in \mathcal{I}_{\text{II}}^-} P\left(\tilde{T}_{\text{II}}^-(u_2) \cap (v_j - b, v_j + b) \neq \emptyset\right) \right].\end{aligned} \quad (28)$$

For random thresholds \tilde{u}_I and \tilde{u}_{II} defined in (14) and (22) respectively, the FDR is

$$\text{FDR}_{\text{III,BH}} = \mathbb{E} \left\{ \frac{V_{I \setminus II}(\tilde{u}_I) + V_{II}(\tilde{u}_{II})}{[R_{I \setminus II}(\tilde{u}_I) + R_{II}(\tilde{u}_{II})] \vee 1} \right\}.$$

Similarly, the corresponding power, denoted by $\text{Power}_{\text{III,BH}}$, is defined as (28) with u_1 and u_2 replaced by \tilde{u}_I and \tilde{u}_{II} respectively.

Theorem 3. *Suppose $y(t)$ contains J_1 Type I change points and J_2 Type II change points ($J = J_1 + J_2$), conditions (C1) and (C2) hold, and $J_1/L \rightarrow A_1 > 0$ and $J_2/L \rightarrow A_2 > 0$ as $L \rightarrow \infty$.*

(i) *If Algorithm 3 is applied with fixed thresholds u_1 and u_2 for Type I and Type II change points respectively, then*

$$\begin{aligned} \limsup \text{FDR}_{\text{III}}(u_1, u_2) &\leq \\ &\frac{E[\tilde{m}_{z_\gamma'}(U(1), u_1)](1 - 2c\gamma A_1) + E[\tilde{m}_{z_\gamma'}(U(1), u_2)](1 - 2c\gamma A_2)}{E[\tilde{m}_{z_\gamma'}(U(1), u_1)](1 - 2c\gamma A_1) + E[\tilde{m}_{z_\gamma'}(U(1), u_2)](1 - 2c\gamma A_2) + A}, \end{aligned} \quad (29)$$

$$\text{Power}_{\text{III}}(u_1, u_2) \rightarrow 1. \quad (30)$$

(ii) *If Algorithm 3 is applied with random thresholds \tilde{u}_I and \tilde{u}_{II} for Type I and Type II change points respectively, then*

$$\limsup \text{FDR}_{\text{III,BH}} \leq \alpha, \quad (31)$$

$$\text{Power}_{\text{III,BH}} \rightarrow 1. \quad (32)$$

3.4 Gaussian auto-correlation model and peak height distribution

Let $X(t)$ be a centered smooth stationary Gaussian process with variance σ^2 . Note that, due to the stationarity, $E(X(t)X''(t)) = -\text{Var}(X'(t))$. Define

$$\eta = -\text{Corr}(X(t), X''(t)) = \frac{\text{Var}(X'(t))}{\sqrt{\text{Var}(X(t))\text{Var}(X''(t))}}.$$

Let $F_X(x)$ denote the right tail probability of $X(t)$ at the local maximum, then

$$\begin{aligned} F_X(x) &= P(X(t) > x \mid t \text{ is a local maximum of } X(t)) \\ &= 1 - \Phi\left(\frac{x}{\sigma\sqrt{1-\eta^2}}\right) + \sqrt{2\pi}\eta\phi\left(\frac{x}{\sigma}\right)\Phi\left(\frac{\eta x}{\sigma\sqrt{1-\eta^2}}\right). \end{aligned} \quad (33)$$

Note that (33) is a general version of the peak height distribution derived in Schwartzman et al. (2011) and Cheng and Schwartzman (2015). One important and appealing characteristic of (33) is that it only depends on the negative correlation between itself and its second derivative, i.e., η .

We consider a simple example of $X(t)$. Let noise $z(t)$ be

$$z(t) = \int_{\mathbb{R}} \frac{1}{\nu} \phi\left(\frac{t-s}{\nu}\right) dB(s), \quad \nu > 0, \quad (34)$$

where $dB(s)$ is Gaussian white noise ($z(t)$ is regarded by convention as Gaussian white noise when $\nu = 0$). Convolving with a Gaussian kernel $w_\gamma(t) = (1/\gamma)\phi(t/\gamma)$ with $\gamma > 0$ produces a zero-mean infinitely differentiable stationary ergodic Gaussian field

$$z_\gamma(t) = \int_{\mathbb{R}} w_\gamma(t-x)z(x)dx = \int_{\mathbb{R}} \frac{1}{\xi} \phi\left(\frac{t-s}{\xi}\right) dB(s), \quad \xi = \sqrt{\gamma^2 + \nu^2}. \quad (35)$$

Lemma 3. *For the smoothed stationary Gaussian process $z_\gamma(t)$, defined in (35), the variance of its derivatives are*

$$\begin{aligned} \text{Var}(z'_\gamma(t)) &= \frac{1}{4\sqrt{\pi}\xi^3}, & \text{Var}(z''_\gamma(t)) &= \frac{3}{8\sqrt{\pi}\xi^5}, \\ \text{Var}(z^{(3)}_\gamma(t)) &= \frac{15}{16\sqrt{\pi}\xi^7}, & \text{Var}(z^{(4)}_\gamma(t)) &= \frac{105}{32\sqrt{\pi}\xi^9}. \end{aligned}$$

Combining Lemma 3 and (33), we immediately have the following proposition:

Proposition 2. *Let $z_\gamma(t)$ be defined in (35). The peak height distribution of $z'_\gamma(t)$ is*

$$F_{z'_\gamma}(x) = 1 - \Phi\left(\frac{x}{\sigma_1\sqrt{1-\eta_1^2}}\right) + \sqrt{2\pi}\eta_1\phi\left(\frac{x}{\sigma_1}\right)\Phi\left(\frac{\eta_1x}{\sigma_1\sqrt{1-\eta_1^2}}\right), \quad (36)$$

where $\eta_1 = \frac{\sqrt{3}}{\sqrt{5}}$ and $\sigma_1^2 = \frac{1}{4\sqrt{\pi}\xi^3}$.

The peak height distribution of $z''_\gamma(t)$ is

$$F_{z''_\gamma}(x) = 1 - \Phi\left(\frac{x}{\sigma_2\sqrt{1-\eta_2^2}}\right) + \sqrt{2\pi}\eta_2\phi\left(\frac{x}{\sigma_2}\right)\Phi\left(\frac{\eta_2x}{\sigma_2\sqrt{1-\eta_2^2}}\right), \quad (37)$$

where $\eta_2 = \frac{\sqrt{5}}{\sqrt{7}}$ and $\sigma_2^2 = \frac{3}{8\sqrt{\pi}\xi^5}$.

3.5 SNR and optimal bandwidth γ

Intuitively, a higher SNR facilitates the detection of change points as it enhances the contrast between the signal and the noise. On the other hand, SNR is not only associated with the size of slope change and jump, but also a function of bandwidth γ . Thus, it is important to study the SNR when choosing the best bandwidth. The SNR of the two types of change points are defined as follows.

Lemma 4. *Assume $z(t)$ is Gaussian white noise ($\nu = 0$ in (35)). For a Type I change point v_j , the SNR is calculated as*

$$\text{SNR}_I(v_j) = \frac{|\mu''_\gamma(v_j)|}{\sqrt{\text{Var}(z''_\gamma(v_j))}} = \frac{\left|\frac{k_{j+1}-k_j}{\sqrt{2\pi}\gamma}\right|}{\sqrt{\frac{3}{8\sqrt{\pi}\gamma^5}}} = \frac{2\gamma^{3/2}}{\sqrt{3}\pi^{1/4}}|k_{j+1}-k_j|. \quad (38)$$

For a Type II change point v_j , it becomes a local extremum at v_j if $a_j \rightarrow \infty$ and $q_j \rightarrow 0$, and the corresponding SNR is calculated as

$$\text{SNR}_{\text{II}}(v_j) = \frac{|\mu'_\gamma(v_j)|}{\sqrt{\text{Var}(z'_\gamma(v_j))}} = \frac{|\frac{a_j}{\sqrt{2\pi}\gamma} + \frac{k_j+k_{j+1}}{2}|}{\sqrt{\frac{1}{4\sqrt{\pi}\gamma^3}}} = \left| \frac{\sqrt{2}a_j}{\pi^{1/4}} \sqrt{\gamma} + (k_j + k_{j+1})\pi^{1/4}\gamma^{3/2} \right|. \quad (39)$$

It is seen from (38) and (39) that SNR is increasing in slope change (absolute value) and jump size. In addition, Lemma 4 shows the SNR is increasing in γ for both Type I and Type II change points. Therefore, if the minimal distance of neighbouring change points d is large enough, a large γ is preferable (see figure 5). However, for a fixed d , to avoid the overlap of two neighbouring smoothed signal segments, such as $(v_j - c\gamma, v_j + c\gamma)$ and $(v_{j+1} - c\gamma, v_{j+1} + c\gamma)$, γ can not be too large, such as $2c\gamma \leq d$.

4 Simulation Study

4.1 Simulation settings

In this section, we will study the performance of our method for different scenarios of the signals. The signals follow the form $\mu(t) = c_j + k_j t$, where $t = 1, \dots, L$. The true change point locations are $v_j = jd$ for $j = 1, \dots, \lfloor L/d \rfloor - 1$, and $d = 150$ is the distance between any two neighboring change points. We consider four different scenarios for the signals: (1) piecewise linear mean with continuous change points (Type I change points); (2) piecewise constant mean with jumps (special case of Type II change points); (3) piecewise linear mean with discontinuous change points (Type II change points); (4) mixture of Type I and Type II change points. For the first three scenarios, we consider $L = 15,000$ and thus $J = 99$ for each scenario. For the mixture case, we consider $L = 30,000$ and $J_1 = J_2 = 99$.

The noise is generated from a zero-mean stationary ergodic Gaussian process. It is a white noise when $\nu = 0$, and correlated when $\nu > 0$. For smoothing, we use the Gaussian kernel $w_\gamma(t) = (1/\gamma)\phi(t/\gamma)\mathbb{1}(t \in [-6\gamma, 6\gamma])$. To control the FDR, the Benjamini-Hochberg (BH) procedure is applied at level of $\alpha = 0.05$. The performance evaluation results are averaged over 1,000 replications.

4.2 Performance of our method

In Section 2, we presented theoretical results of FDR and power of our method. In this section, we will further validate these properties through numerical studies.

Figure 5 shows the performance of our method for the four different scenarios of signals. It is seen that as the SNR increases, the FDR converges to its asymptotic limit, which is below the FDR control level of $\alpha = 0.05$, and the power approaches 1. For a fixed bandwidth γ , a higher SNR implies a larger slope change or jump size, which is corresponding with the conditions (C1) and (C2) respectively. It is worth noting that the two conditions in our theoretical analysis assume an

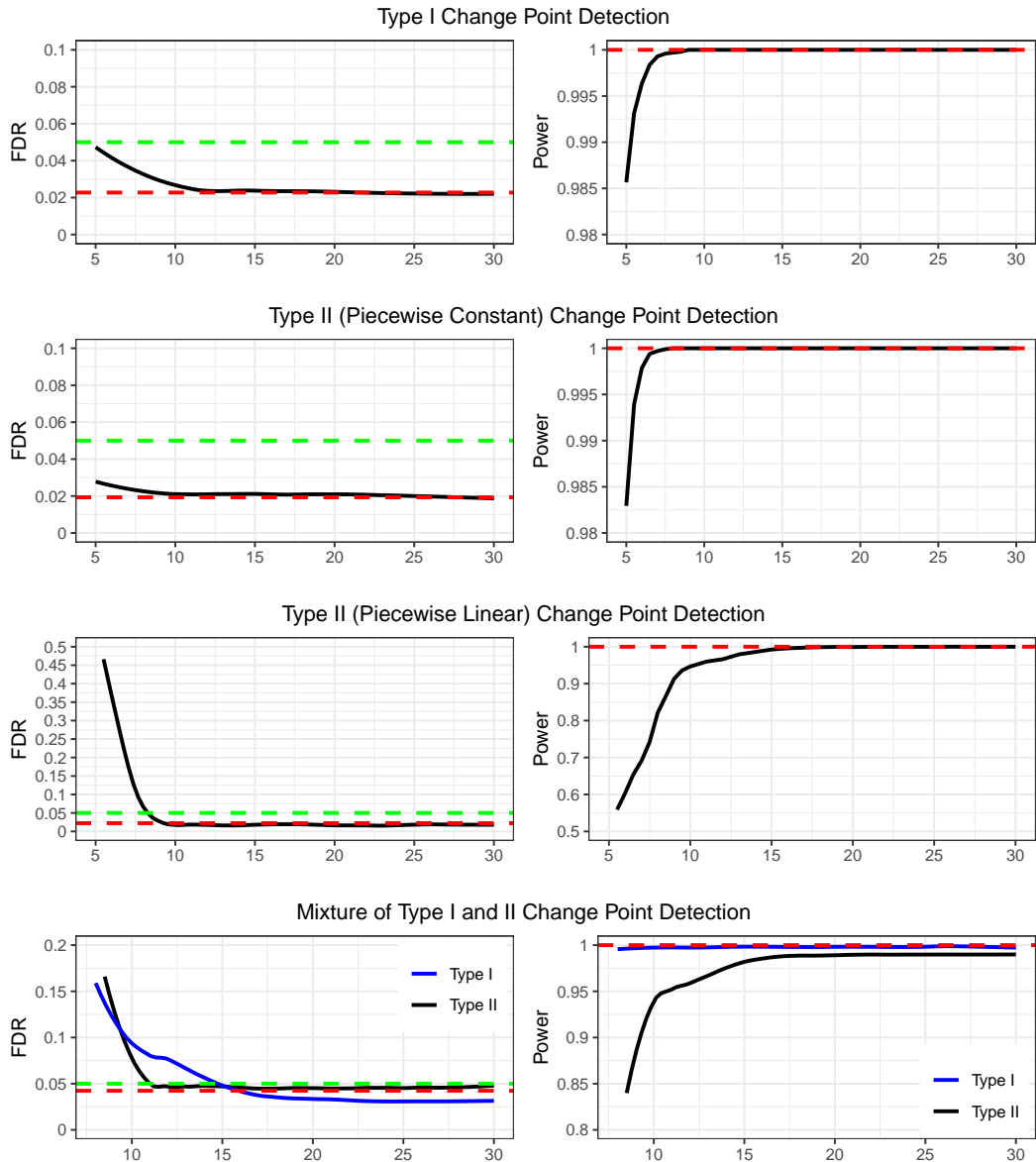


Figure 5: The FDR (left panel) and power (right panel) versus SNR for change point detection of different types of signals. In this example, the kernel bandwidth is $\gamma = 10$ and the location tolerance is $b = 10$. The red dashed lines indicate the asymptotic limits of FDR and power. The green dashed lines indicate the significant level $\alpha = 0.05$.

infinite SNR. However, our numerical results demonstrate that even when SNR is not too large (SNR is around 15 in our simulation), both the FDR and Power have already converged to their asymptotic results.

4.2.1 Choice of bandwidth γ

Figure 6 illustrates the results of the FDR and power as the kernel bandwidth γ increases. When γ is not sufficiently large, the performance of FDR and power improves as γ increases. This is because a larger γ implies a larger SNR, resulting in more accurate change point detection and a higher power to detect true change points while controlling the FDR. However, there is a trade-off. If γ becomes too large, it can lead to the issue of overlap. For example, the kernel region, defined by 12γ , becomes longer than the distance between neighboring change points v_j and v_{j+1} . This overlap can introduce distortions and complicate the detection of individual change points. Therefore, in our simulation cases, $\gamma = 12$ is recommended.

4.3 Comparison with other methods

In the comparison of different change point detection methods, we evaluated the accuracy and computing time of change point detection. Both short-term (see the section 4.1) and long-term data sequence were considered. The long-term data sequence is generated by repeating the short-term data (ten times in our simulation), ensuring that the patterns in both data sequences are the same.

We compared our method with some multiple testing-based change point detection methods: B&P (Bai, 1997), NOT (Baranowski et al., 2019), and NSP (Fryzlewicz, 2023). Note that due to the extremely long computing time required by the BP method, we excluded the results of BP method from the long-term data comparison. For the NSP method, change points were estimated as confidence intervals, and we used the midpoints of these intervals as point estimates for comparison with other methods (same as in the section 5). Additionally, the scenario of mixture of Type I and Type II change points was not considered, because the other three methods can not distinguish between Type I and Type II change points.

Suppose and the number of true change points is J , and the number of detected change points is \hat{J} . For any detected change point \hat{v}_i , $i = 1, 2, \dots, \hat{J}$, it is defined as the estimate of the true change point v_j such that

$$j = \operatorname{argmin}_{j=1,2,\dots,J} |\hat{v}_i - v_j| \quad (40)$$

For simplicity, let $v_i^0 = v_j$ be the true change point corresponding to \hat{v}_i , where j is defined in (40). Note that one true change point may correspond to multiple estimated change points. The detection accuracy of \hat{v}_i is measured using the distance of $|\hat{v}_i - v_i^0|$ for $i = 1, 2, \dots, \hat{J}$, which is represented by the capture rate in Tables 1 and 2.

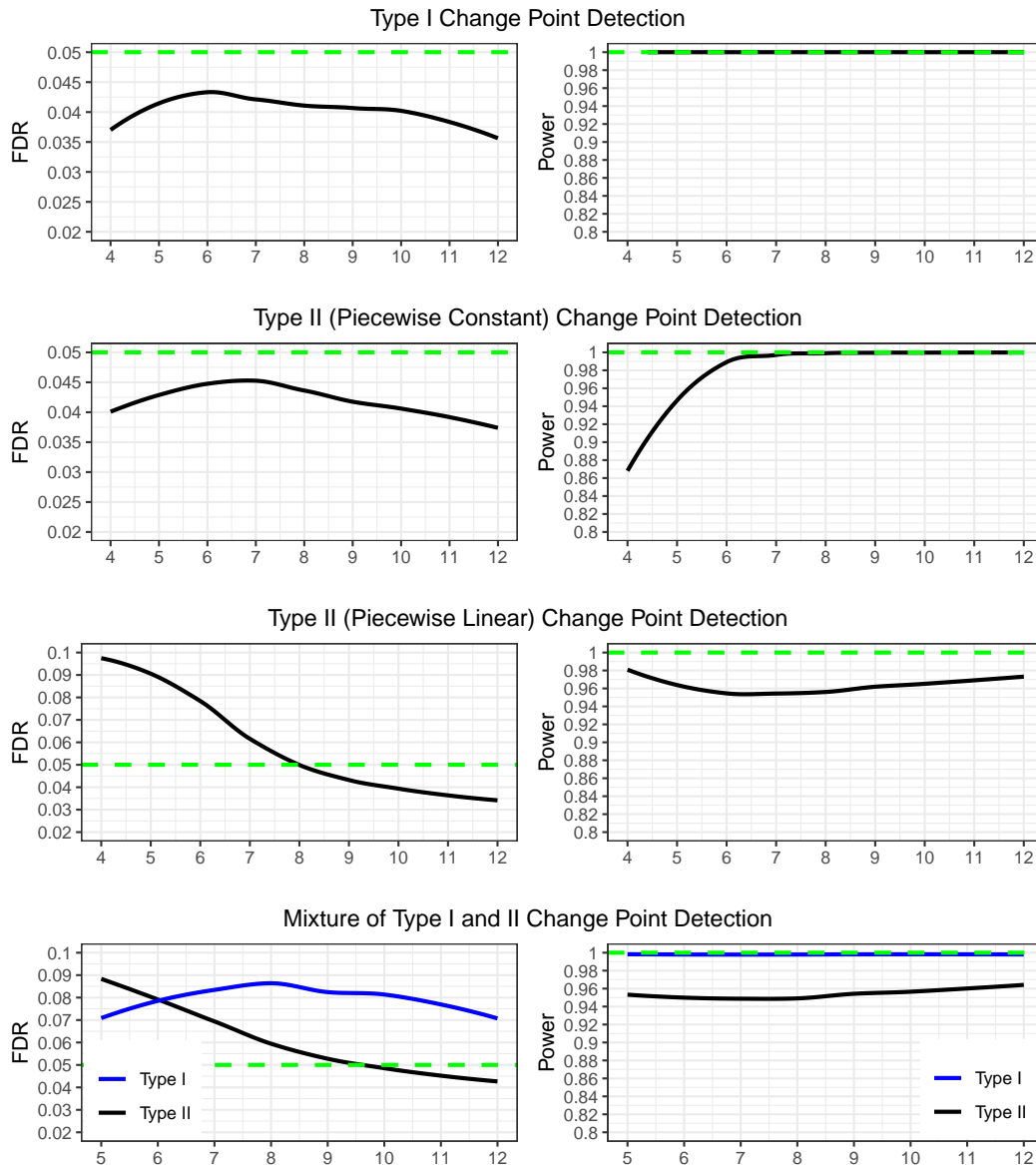


Figure 6: The FDR (left panel) and Power (right panel) versus the bandwidth γ for change point detection of different types of signals. In this example, the kernel bandwidth γ varies from 4 to 12 and the location tolerance is $b = 10$. The green dashed lines indicate the FDR control level $\alpha = 0.05$ for FDR plots and 1 for power plots .

Table 1 displays the results for short-term data, showing that our proposed method, NOT and NSP exhibit excellent performance in terms of FDR control and power for all the scenarios. Both NOT and our method can achieve high accuracy rate of change point detection within one γ , and our method is the fastest among the algorithms considered. In Table 2, it is seen that for the long-term data sequence, NOT and NSP do not perform well regarding the FDR control, Power and detection accuracy. But our method maintains excellent performance and the advantage of having the smallest computing time.

It is worth noting that our method performs a little better in terms of FDR and power in the long-term data than than in the short-term data, because of the asymptotic conditions $L \rightarrow \infty$ and $J/L \rightarrow A > 0$. Additionally, the smallest computing time of our method in both short-term and long-term data sequences demonstrates that our method has the lowest computation complexity.

Table 1: Detection accuracy of change points for the short-term data sequence ($\gamma = 10$ and $b = \gamma$). The capture rate of an interval I is defined as $\sum_{i=1}^J \mathbb{1}(|\hat{v}_i - v_i^0| \in I)/J$.

Signal Type	Method	Capture rate of interval					FDR	Power	Time (s)
		$[0, \frac{1}{3}\gamma)$	$[\frac{1}{3}\gamma, \gamma)$	$[\gamma, 2\gamma)$	$[2\gamma, 4\gamma)$	$\geq 4\gamma$			
Type I	mSTEM	0.8400	0.1533	0.0217	0.0267	0.0483	0.0125	0.9933	0.1370
	NOT	0.9883	0.0117	0.0000	0.0017	0.0000	0.0572	1.0000	1.3550
	NSP	0.6183	0.1900	0.1617	0.0300	0.0000	0.0458	0.9999	3.2417
	B&P	0.4700	0.5083	0.0217	0.0000	0.0000	0.1632	0.9783	87.4562
Type II Piecewise Constant	mSTEM	0.9617	0.0383	0.0000	0.0367	0.0333	0.0227	1.0000	0.0290
	NOT	0.9833	0.0183	0.0017	0.0000	0.0017	0.0558	1.0000	0.2863
	NSP	0.6767	0.3133	0.2117	0.0867	0.0100	0.0517	0.9001	1.9430
	B&P	0.4117	0.0233	0.0467	0.2050	0.0000	0.1260	0.4350	71.0924
Type II Piecewise Linear	mSTEM	0.9983	0.0017	0.0000	0.0067	0.0233	0.0348	1.0000	0.0839
	NOT	0.8833	0.0933	0.0233	0.0000	0.0000	0.0727	0.9766	0.4524
	NSP	0.6967	0.2417	0.0333	0.0283	0.0000	0.0626	0.9384	2.8013
	B&P	0.3333	0.0000	0.3015	0.3333	0.0745	0.1633	0.3333	68.3345

5 Data examples

In this section, we applied our method to real applications and compared with NOT and NSP (BP method was excluded due to its weak performance and large computing time). Two datasets were considered: one is global temperature records (short-term), another is the stock price of a hotel company (long-term). We evaluated the performance of all the three methods on these datasets.

Table 2: Detection accuracy of change points for the long-term data sequence ($\gamma = 10$ and $b = \gamma$). The proportion of an interval I is defined as $\sum_{i=1}^J \mathbb{1}(|\hat{v}_i - v_i^0| \in I)/J$.

Signal Type	Method [†]	Capture rate of interval					FDR	Power	Time (s)
		$[0, \frac{1}{3}\gamma)$	$[\frac{1}{3}\gamma, \gamma)$	$[\gamma, 2\gamma)$	$[2\gamma, 4\gamma)$	$\geq 4\gamma$			
Type I	mSTEM	0.7616	0.2241	0.0295	0.0244	0.0135	0.0127	0.9963	0.2469
	NOT	0.1358	0.1712	0.2475	0.5028	0.2369	0.0853	0.8732	112.5007
	NSP	0.3512	0.4607	0.1692	0.0086	0.0000	0.0792	0.8362	433.6193
Type II Piecewise Constant	mSTEM	0.9702	0.0000	0.000	0.0154	0.0161	0.01463	1.0000	0.1188
	NOT	0.8633	0.0037	0.007	0.0177	0.0090	0.0735	0.9164	48.4487
	NSP	0.6398	0.3202	0.030	0.0000	0.0000	0.08011	0.9228	213.0398
Type II Piecewise Linear	mSTEM	0.9899	0.0000	0.0000	0.0065	0.0133	0.0237	0.9992	1.0627
	NOT	0.8748	0.0002	0.0009	0.0032	0.0025	0.1217	0.8012	10.6064
	NSP	0.6059	0.3543	0.0298	0.0000	0.0000	0.1383	0.8255	400.6633

[†] B&P method was not included due to its substantial computational time requirements.

5.1 Global temperature records

Climate change research plays a vital role in addressing the impacts of global warming and informing policy decisions related to mitigation and adaptation strategies. The analysis of temperature change can provide is crucial in understanding the patterns and changes in climate over time.

In this paper, we studied the data of global mean land-ocean temperature deviations (from the average temperature between the year 1951 and the year 1980), measured in degrees centigrade, for the year from 1880 to 2015. The data is available at <https://data.giss.nasa.gov/gistemp/graphs>.

Figure 7 illustrates the results of applying all the three methods to the global temperature data. Our method detected two Type II change points at 1902 and 1934, as well as one Type I change point at 1971. These findings are consistent with the results presented in Yu and Ruggieri (2019), where they analyzed five time series and identified three distinct periods of significant temperature change during the 20th century. Specifically, their study reported change points between 1902-1917, 1936-1945 and 1963-1976. Indeed, the result of our detection method aligns with the visual assessment of the data sequence. The observed pattern suggests that the signal remains relatively constant during the first period (1880 - 1902), followed by a linear trend in the second period (1903 - 1934), then a another constant signal in the third period (1935 - 1971), and finally a linear trend in the last period.

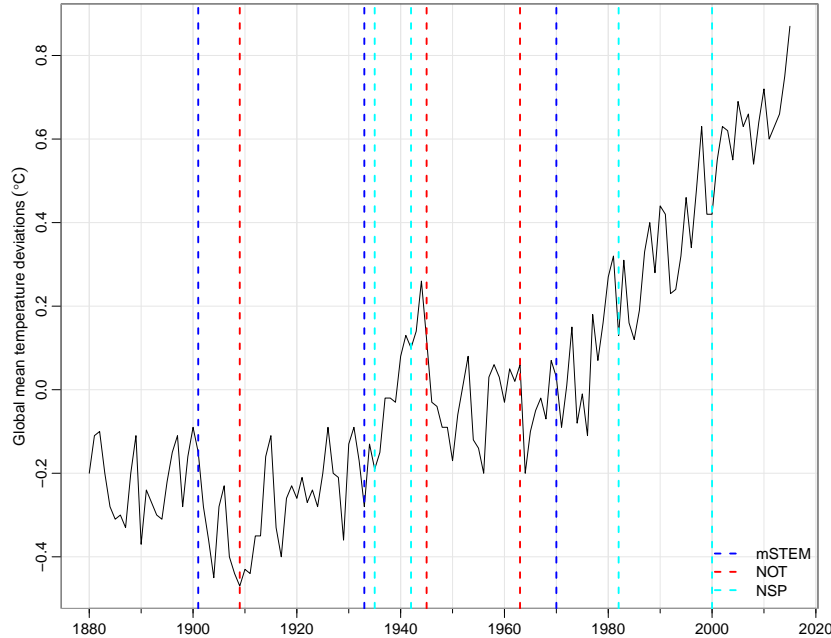


Figure 7: Change point detection of global mean land-ocean temperature deviations for the year from 1880 to 2015. Our method detects three change points: 1902 (Type II), 1934 (Type II) and 1971 (Type I); NOT detects three change points: 1910, 1946 and 1964; NSP detects three change points: 1936, 1943, 1983 and 2001.

5.2 Stock price of Host Hotel & Resorts, Inc.

Analyzing the daily stock price of Host Hotel & Resorts, Inc. (HST) from January 1, 2018, to November 5, 2021, one can provide valuable insights into the company’s stock performance and detect any significant change points that may have occurred during this period. As the world’s largest lodging and real estate investment trust (REIT), HST’s stock price can be influenced by various factors, including market conditions, industry trends, company-specific events, and macroeconomic factors. The historical data for HST stock price is available at <https://finance.yahoo.com>.

By applying our method to detect change points in the HST stock price, one can identify periods of significant shifts in the stock’s behavior or trends. These change points may correspond to events or factors that impacted HST’s stock price, such as earnings releases, mergers and acquisitions, changes in industry regulations, or other market-moving news.

Figure 8 shows the detection results for the HST stock price. It is seen that NOT and NSP (especially NSP) tend to be sensitive to variations in the time series, leading to the detection of more local extrema that may be attributed to noise. This can result in a higher FDR. In contrast, our method provides detection results that can be interpreted reasonably. The detected change points align with

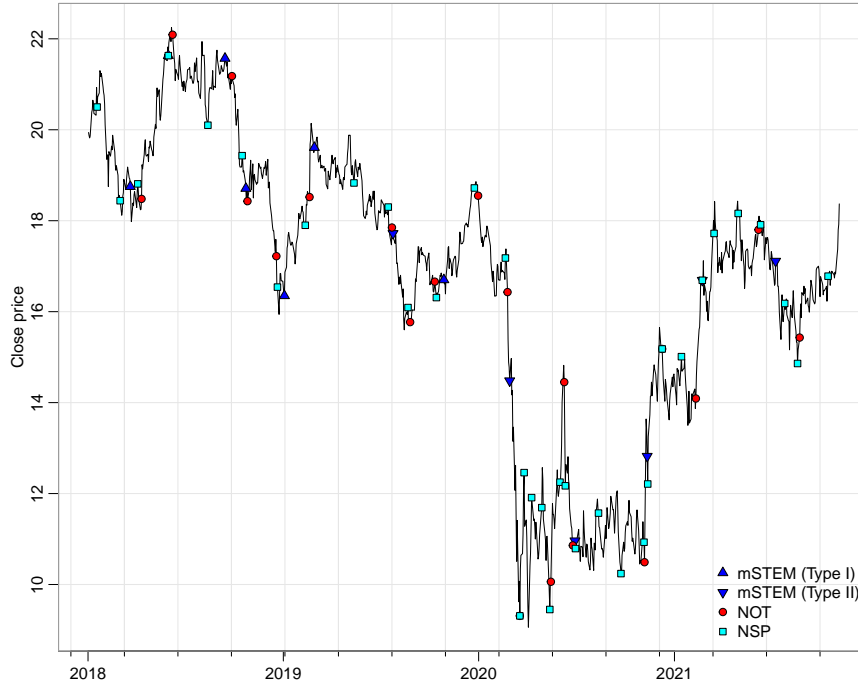


Figure 8: Change point detection of HST stock price (January 1, 2018 – November 5, 2020).

big events such as the outbreak of trade war between the USA and China in 2018 – 2019, which impacted the S&P 500 and other large-cap stocks. Similarly, the detected change points after 2020 correspond to the timeline of the Covid-19 outbreak, which has a profound impact on the global tourist industry.

6 Discussion

6.1 Choice of smoothing bandwidth γ

The choice of the smoothing bandwidth γ is indeed an important aspect of change point detection. It plays a role in balancing the trade-off between overlapping of the smoothed signal supports and accuracy of detecting change points. Thus, either a small γ (if the noise is highly autocorrelated) or a relatively large γ (if the noise is less autocorrelated) is preferred in order to increase power, but only to the extent that the smoothed signal supports have little overlap. Considering the Gaussian kernel with support domain of $\pm c\gamma$, an initial guideline for choosing γ can be set as $b = d/(2c)$, where d is the minimal distance between any two neighboring change points. This guideline ensures that the supports of the smoothed signals do not overlap excessively. For example, if we consider the Gaussian kernel to have an effective support of $\pm 4\gamma$ and $d = 100$, we may choose γ to be no larger

than $\gamma = 12$.

It is worth noting that the choice of γ may require an iterative procedure, especially when the distance between change points is unknown. A more precise optimization needs to be performed by iteratively adjusting the value of γ and evaluating the detection performance. Moreover, in some cases where the change points are not uniformly distributed and some are close together while others are far apart, an adaptive bandwidth that varies across the signal may be preferable to effectively capture both closely spaced and widely spaced change points. We leave these as problems for future research.

6.2 Type II change points with moderate $|q_j|$

For a Type II change point v_j , we have studied in this paper the case of small $|q_j|$, and showed in Remark 2 the case of large $|q_j|$ that it behaves similarly to a Type I change point. But when a Type II change point has moderate $|q_j|$, for example $|q_j|$ is close to c/γ , the first derivative $\mu'_\gamma(t)$ can produce a local extremum at $t = v_j + \gamma^2|q_j| \approx v_j + c\gamma$ or $t = v_j - \gamma^2|q_j| \approx v_j - c\gamma$, which is near the endpoints of the smoothed signal region and outside of $v_j \pm b$. This may lead to false detection of a significant peak resulting from noise instead of a true change point, leading to overestimation of FDR and underestimation of power.

The asymptotic theories presented in Section 3 demonstrate FDR control and power consistency for Type II change points ($a_j = 0$, or $a_j \neq 0$ but $|q_j| \rightarrow \infty$) and Type II change points with $|q_j| \rightarrow 0$. But for Type II change points with q_j being a fixed number close to c/γ , by (39) SNR goes to infinity as $a_j \rightarrow \infty$. Thus these change points with moderate $|q_j|$ would be falsely detected as significant peaks resulting from random noise.

Addressing this limitation of detecting Type II change points with moderate $|q_j|$ would be an important question for future research. It may involve developing additional theoretical insights and modifying our proposed method mSTEM to enhance its ability to handle a wider range change points scenarios.

6.3 Extension to multivariate linear models

A univariate linear model is assumed to formulate the signal-plus-noise in this paper, but our proposed method can be extended to the multivariate linear models (Bai and Safikhani, 2022; Chen and Gupta, 2012). For example, we are interested in the following p -dimensional linear model and detecting possible change points:

$$y_t = \mu_t + z_t = X_t \boldsymbol{\beta}^{(j)} + z_t, \text{ for } t \in (v_{j-1}, v_j], j = 1, 2, \dots \quad (41)$$

where $X_t = (1, X_{1t}, \dots, X_{pt})^T$ is the covariate vector and $\boldsymbol{\beta}^{(j)} = (\beta_0^{(j)}, \beta_1^{(j)}, \dots, \beta_p^{(j)})^T \in \mathbb{R}^{p+1}$. When $p = 1$, by letting $\boldsymbol{\beta}^{(j)} = (\beta_0^{(j)}, \beta_1^{(j)})^T = (c_j, k_j)^T$ for $t \in (v_{j-1}, v_j], j = 1, 2, \dots$, and $X_{1t} = t$, (41) becomes the univariate piecewise linear model $y_t = c_j + k_j t + z_t$.

To estimate the number and location of change points simultaneously, our mSTEM method can still be applied to each dimension independently. Specifically, suppose we have T realizations $\{(y_t, X_t), t = 1, \dots, T\}$, for each dimension m , $m = 1, \dots, p$, the first and second derivatives of $\mu_{\gamma t}$ are studied, and suppose the detected change points are $\mathbf{v}^{(m)} = (v_1^{(m)}, \dots, v_{n_m}^{(m)})$, where n_m is the number of detected change points for the m -th dimension. It is possible that some change points occur at similar or exactly the same locations across different dimensions. For example, in dimension i and j , $i \neq j$, some locations in $\mathbf{v}^{(i)}$ and $\mathbf{v}^{(j)}$ will be very close, we consider these change points to be the result of the same underlying change points.

6.4 Nonstationary Gaussian noise

In this paper, the Gaussian noise is assumed to be stationary, which allows the error terms can be correlated. However, in real applications, it is common that the data contains nonstationary Gaussian noise (Heinonen et al., 2016; Phoon et al., 2005). Thus, it is interesting and valuable to investigate change point detection under nonstationary Gaussian noise. To achieve this, we will study the peak height distribution for nonstationary Gaussian noise and show the FDR control and power consistency under certain assumptions, which would be promising but with certain challenges.

Supplementary Materials

The supplementary materials contain proofs of all technical results in the paper.

Acknowledgements

The authors thank professor Armin Schwartzman (University of California San Diego) for helpful discussions and suggestions.

Funding

Dan Cheng acknowledges support from National Science Foundation grant DMS-2220523 and Simons Foundation Collaboration Grant 854127.

Supplementary Materials

A Proofs in Section 2

Proof of Lemma 1. Recall that $w_\gamma(t)$ defined in equation (3) is a truncated Gaussian kernel with support $[-c\gamma, c\gamma]$ and bandwidth γ . For $t \in (v_j - c\gamma, v_j + c\gamma)$, we have

$$\begin{aligned}
 \mu_\gamma(t) &= w_\gamma(t) * \mu(t) = \int_{t-c\gamma}^{t+c\gamma} w_\gamma(t-s)\mu(s)ds \\
 &= \int_{t-c\gamma}^{v_j} \frac{1}{\gamma} \phi\left(\frac{t-s}{\gamma}\right)(c_j + k_j s)ds + \int_{v_j}^{t+c\gamma} \frac{1}{\gamma} \phi\left(\frac{t-s}{\gamma}\right)(c_{j+1} + k_{j+1} s)ds \\
 &= \int_{-c}^{\frac{v_j-t}{\gamma}} \phi(x)(c_j + k_j t + k_j \gamma x)dx + \int_{\frac{v_j-t}{\gamma}}^c \phi(x)(c_{j+1} + k_{j+1} t + k_{j+1} \gamma x)dx \\
 &= [c_j + k_j t - (c_{j+1} + k_{j+1} t)]\Phi\left(\frac{v_j-t}{\gamma}\right) + [c_j + k_j t + (c_{j+1} + k_{j+1} t)]\Phi(c) - (c_j + k_j t) \\
 &\quad + (k_j - k_{j+1})\gamma\phi(c) + (k_{j+1} - k_j)\gamma\phi\left(\frac{v_j-t}{\gamma}\right).
 \end{aligned} \tag{A.42}$$

Similarly, we obtain that, for $t \in (v_j + c\gamma, v_{j+1} - c\gamma)$,

$$\begin{aligned}
 \mu_\gamma(t) &= w_\gamma(t) * \mu(t) = \int_{t-c\gamma}^{t+c\gamma} \frac{1}{\gamma} \phi\left(\frac{t-s}{\gamma}\right)(c_{j+1} + k_{j+1} s)ds \\
 &= (c_{j+1} + k_{j+1} t)[2\Phi(c) - 1];
 \end{aligned} \tag{A.43}$$

and for $t \in (v_{j-1} + c\gamma, v_j - c\gamma)$,

$$\begin{aligned}
 \mu_\gamma(t) &= w_\gamma(t) * \mu(t) = \int_{t-c\gamma}^{t+c\gamma} \frac{1}{\gamma} \phi\left(\frac{t-s}{\gamma}\right)(c_j + k_j s)ds \\
 &= (c_j + k_j t)[2\Phi(c) - 1].
 \end{aligned} \tag{A.44}$$

Taking the first and second derivatives of $\mu_\gamma(t)$ in (A.42), (A.43) and (A.44) respectively, we obtain

$$\mu'_\gamma(t) = \begin{cases} \frac{a_j}{\gamma} \phi\left(\frac{v_j-t}{\gamma}\right) + (k_j - k_{j+1})\Phi\left(\frac{v_j-t}{\gamma}\right) + (k_j + k_{j+1})\Phi(c) - k_j & t \in (v_j - c\gamma, v_j + c\gamma), \\ k_j[2\Phi(c) - 1] & t \in (v_{j-1} + c\gamma, v_j - c\gamma), \\ k_{j+1}[2\Phi(c) - 1] & t \in (v_j + c\gamma, v_{j+1} - c\gamma), \end{cases}$$

and

$$\mu''_\gamma(t) = \begin{cases} \frac{a_j(v_j-t) + (k_{j+1} - k_j)\gamma^2}{\gamma^3} \phi\left(\frac{v_j-t}{\gamma}\right) & t \in (v_j - c\gamma, v_j + c\gamma), \\ 0 & \text{otherwise.} \end{cases}$$

□

Proof of Lemma 2. Note that, if $a_j = 0$, then $\mu'_\gamma(t)$ is monotone in $(v_j - c\gamma, v_j + c\gamma)$ and hence there is no local extremum. If $a_j \neq 0$, by letting $\mu''_\gamma(t) = 0$, we see that the local extremum of $\mu'_\gamma(t)$ is achieved at $t = v_j + \gamma^2 q_j$. Similarly, solving the equation

$$\mu'''_\gamma(t) = \left[\frac{a_j}{\gamma^3} + \frac{a_j(v_j - t) + (k_{j+1} - k_j)\gamma^2}{\gamma^3} \frac{v_j - t}{\gamma^2} \right] \phi\left(\frac{v_j - t}{\gamma}\right) = 0,$$

we obtain that the local extremum of $\mu''_\gamma(t)$ is achieved at

$$t = \begin{cases} v_j + \frac{\gamma^2 q_j \pm \gamma \sqrt{4 + q_j^2 \gamma^2}}{2} & a_j \neq 0, \\ v_j & a_j = 0. \end{cases}$$

□

B Peak Height Distribution for $z'_\gamma(t)$ and $z''_\gamma(t)$

Proof of Lemma 3. Due to the stationarity of $z_\gamma(t)$, without loss of generality, we only consider the case when $t = 0$. The variances of $z_\gamma^{(d)}(t)$, $d = 1, \dots, 4$, are calculated as follows

$$\begin{aligned} \text{Var}(z'_\gamma(0)) &= \int_{\mathbb{R}} \frac{s^2}{\xi^6} \phi^2\left(\frac{s}{\xi}\right) ds \\ &= \frac{1}{\xi^6} \frac{\xi}{2\sqrt{\pi}} \int_{\mathbb{R}} s^2 \frac{\sqrt{2}}{\xi} \phi\left(\frac{s}{\xi/\sqrt{2}}\right) ds \\ &= \frac{1}{\xi^6} \frac{\xi}{2\sqrt{\pi}} \frac{\xi^2}{2} = \frac{1}{4\sqrt{\pi}\xi^3}; \end{aligned}$$

$$\begin{aligned}
\text{Var}(z''_\gamma(0)) &= \int_{\mathbb{R}} \frac{1}{\xi^6} \phi^2\left(\frac{s}{\xi}\right) ds - 2 \int_{\mathbb{R}} \frac{s^2}{\xi^8} \phi^2\left(\frac{s}{\xi}\right) ds + \int_{\mathbb{R}} \frac{s^4}{\xi^{10}} \phi^2\left(\frac{s}{\xi}\right) ds \\
&= \frac{1}{\xi^4} \frac{1}{2\sqrt{\pi}\xi} - \frac{2}{\xi^2} \frac{1}{4\sqrt{\pi}\xi^3} + \frac{1}{\xi^{10}} \frac{\xi}{2\sqrt{\pi}} \int_{\mathbb{R}} s^4 \frac{\xi}{\sqrt{2}} \phi\left(\frac{s}{\xi/\sqrt{2}}\right) ds \\
&= \frac{1}{\xi^{10}} \frac{\xi}{2\sqrt{\pi}} \frac{3\xi^4}{4} = \frac{3}{8\sqrt{\pi}\xi^5}; \\
\text{Var}(z'''_\gamma(0)) &= 9 \int_{\mathbb{R}} \frac{s^2}{\xi^{10}} \phi^2\left(\frac{s}{\xi}\right) ds - 6 \int_{\mathbb{R}} \frac{s^4}{\xi^{12}} \phi^2\left(\frac{s}{\xi}\right) ds + \int_{\mathbb{R}} \frac{s^6}{\xi^{14}} \phi^2\left(\frac{s}{\xi}\right) ds \\
&= \frac{9}{\xi^4} \frac{1}{4\sqrt{\pi}\xi^3} - \frac{6}{\xi^2} \frac{3}{8\sqrt{\pi}\xi^5} + \frac{1}{\xi^{14}} \frac{\xi}{2\sqrt{\pi}} \int_{\mathbb{R}} s^6 \frac{\sqrt{2}}{\xi} \phi\left(\frac{s}{\xi/\sqrt{2}}\right) ds \\
&= \frac{1}{\xi^{14}} \frac{\xi}{2\sqrt{\pi}} \frac{15\xi^6}{8} = \frac{15}{16\sqrt{\pi}\xi^7}; \\
\text{Var}(z^{(4)}_\gamma(0)) &= 9 \int_{\mathbb{R}} \frac{1}{\xi^{10}} \phi^2\left(\frac{s}{\xi}\right) ds - 36 \int_{\mathbb{R}} \frac{s^2}{\xi^{12}} \phi^2\left(\frac{s}{\xi}\right) ds + 42 \int_{\mathbb{R}} \frac{s^4}{\xi^{14}} \phi^2\left(\frac{s}{\xi}\right) ds \\
&\quad - 12 \int_{\mathbb{R}} \frac{s^6}{\xi^{16}} \phi^2\left(\frac{s}{\xi}\right) ds + \int_{\mathbb{R}} \frac{s^8}{\xi^{18}} \phi^2\left(\frac{s}{\xi}\right) ds \\
&= \frac{1}{\xi^9} \left(9 \times \frac{1}{2\sqrt{\pi}} - 36 \times \frac{1}{4\sqrt{\pi}} + 42 \times \frac{3}{8\sqrt{\pi}} - 12 \times \frac{15}{16\sqrt{\pi}} + \frac{1}{2\sqrt{\pi}} \times \frac{105}{16} \right) \\
&= \frac{105}{32\sqrt{\pi}\xi^9}.
\end{aligned}$$

Hence, for the Gaussian process $z'_\gamma(t)$,

$$\eta = \frac{\text{Var}(z''_\gamma(0))}{\sqrt{\text{Var}(z'_\gamma(0))\text{Var}(z'''_\gamma(0))}} = \frac{\sqrt{3}}{\sqrt{5}};$$

and for the Gaussian process $z''_\gamma(t)$,

$$\eta = \frac{\text{Var}(z'''_\gamma(0))}{\sqrt{\text{Var}(z''_\gamma(0))\text{Var}(z^{(4)}_\gamma(0))}} = \frac{\sqrt{5}}{\sqrt{7}}.$$

Therefore, the peak height distribution of $z'_\gamma(t)$ has parameters $\sigma^2 = \frac{1}{4\sqrt{\pi}\xi^3}$ and $\eta = \frac{\sqrt{3}}{\sqrt{5}}$; the peak height distribution of $z''_\gamma(t)$ has parameters $\sigma^2 = \frac{3}{8\sqrt{\pi}\xi^5}$ and $\eta = \frac{\sqrt{5}}{\sqrt{7}}$. \square

C Supporting Results for FDR Control and Power Consistency

Type I change points are detected using the second derivative, $\mu''_\gamma(t)$, which is the derivative of $\mu'_\gamma(t)$. Moreover, $\mu'(t)$ is piecewise constant. Thus the detection of Type I change points using the second derivative is essentially equivalent to the detection of change points in piecewise constant signals

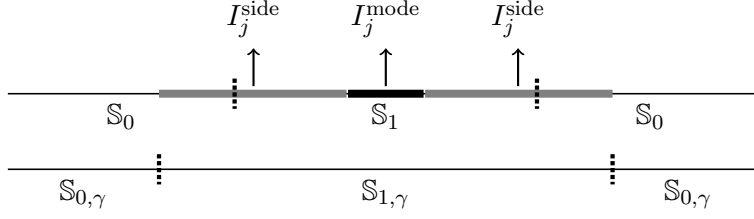


Figure 9: Illustration of the *signal region* \mathbb{S}_1 (S_j in this example), *null region* \mathbb{S}_0 , *smoothed signal region* $\mathbb{S}_{1,\gamma}$ ($S_{j,\gamma}$ in this example) and *smoothed null region* $\mathbb{S}_{0,\gamma}$. I_j^{mode} and I_j^{side} are a partition of $S_{j,\gamma}$ such that $I_j^{\text{mode}} \subset S_j \subset S_{j,\gamma}$.

(Cheng et al., 2020; Schwartzman et al., 2011). The proofs of Theorem 1 can be referred from the works of Cheng et al. (2020) and Schwartzman et al. (2011).

However, for the proofs of Theorem 2 and Theorem 3, we require the following lemmas in this section. It is important to note that the lemmas provided below are based on Type II change points detection, where $a_j \neq 0$.

Recall that the *signal region* is defined as $\mathbb{S}_1 = \cup_{j=1}^J S_j = \cup_{j=1}^J (v_j - b, v_j + b)$, and the smoothed signal is generated by convolving the signal and a kernel function with support $[-c\gamma, c\gamma]$. Hence, the *smoothed signal region* is $\mathbb{S}_{1,\gamma} = \cup_{j=1}^J S_{j,\gamma} = \cup_{j=1}^J (v_j - c\gamma, v_j + c\gamma)$, where $S_{j,\gamma}$ is the smoothed signal region of change point v_j (see Figure 9).

Lemma S1. *Let $S_{j,\gamma} = (v_j - c\gamma, v_j + c\gamma) = I_j^{\text{side}} \cap I_j^{\text{mode}}$ be a partition, where $I_j^{\text{mode}} := \{t \in U(L) : |t - v_j| \leq \delta\}$ and $\delta < \min\{b, \gamma\}$ such that $I_j^{\text{mode}} \subset S_j$. If $q = \sup_j |q_j|$ is sufficiently small, then*

- (1) $M_\gamma = \inf M_{j,\gamma} > 0$, where $M_{j,\gamma} = \frac{\mu'_\gamma(t) - k(t)}{a_j}$ and $k(t) = \mu'(t)$ for $t \in I_j^{\text{mode}}$.
- (2) $C_\gamma = \inf_j C_{j,\gamma} > 0$, where $C_{j,\gamma} = \frac{1}{|a_j|} \inf_{I_j^{\text{side}}} |\mu''_\gamma(t)|$.
- (3) $D_\gamma = \inf_j D_{j,\gamma} > 0$, where $D_{j,\gamma} = \frac{1}{|a_j|} \inf_{I_j^{\text{mode}}} |\mu'''_\gamma(t)|$.

Proof. (1). By the arguments of Lemma 1, it follows that

$$\begin{aligned}
M_{j,\gamma} &= \frac{\mu'_\gamma(t) - k(t)}{a_j} \\
&= \frac{1}{a_j} \left[\frac{a_j}{\gamma} \phi\left(\frac{v_j - t}{\gamma}\right) - (k_{j+1} - k_j) \Phi\left(\frac{v_j - t}{\gamma}\right) + k_{j+1} \right] - \frac{k(t)}{a_j} \\
&= \frac{1}{\gamma} \phi\left(\frac{v_j - t}{\gamma}\right) - q_j \Phi\left(\frac{v_j - t}{\gamma}\right) + \frac{k_{j+1} - k(t)}{a_j}.
\end{aligned}$$

For $t \in I_j^{\text{mode}}$, $(k_{j+1} - k(t))/a_j = 0$ or q_j as $k(t) = k_j$ or k_{j+1} . If q is sufficiently small, then $M_{j,\gamma} > 0$ and it follows that $M_\gamma = \inf M_{j,\gamma} > 0$.

(2). Since for $t \in I_j^{\text{side}} \subset S_{j,\gamma}$ implies $\delta < |v_j - t| < c\gamma$, we obtain

$$\begin{aligned} C_{j,\gamma} &= \frac{1}{|a_j|} \inf_{I_j^{\text{side}}} |\mu_\gamma''(t)| \\ &= \inf_{I_j^{\text{side}}} \left| \frac{(v_j - t) + q_j \gamma^2}{\gamma^3} \phi\left(\frac{v_j - t}{\gamma}\right) \right|. \end{aligned}$$

If q is sufficiently small, then $C_{j,\gamma} > 0$ and $C_\gamma = \inf_j C_{j,\gamma} > 0$.

(3). For $t \in I_j^{\text{mode}}$, we have

$$\begin{aligned} D_{j,\gamma} &= \frac{1}{|a_j|} \inf_{I_j^{\text{mode}}} |\mu_\gamma'''(t)| \\ &= \inf_{I_j^{\text{mode}}} \left| \frac{1}{\gamma^3} + \frac{(v_j - t)^2 + q_j(v_j - t)\gamma^2}{\gamma^5} \phi\left(\frac{v_j - t}{\gamma}\right) \right|. \end{aligned}$$

If q is sufficiently small, then $D_{j,\gamma} > 0$ and $D_\gamma = \inf_j D_{j,\gamma} > 0$. □

Lemma S2. For a Type II change point v_j , suppose that $q = \sup_j |q_j|$ is sufficiently small, then $\mu_\gamma'(t)$ has a local maximum/minimum at $t = v_j + \gamma^2 q_j \in I_j^{\text{mode}}$. Define $\sigma_1 = sd(z_\gamma'(t))$, $\sigma_2 = sd(z_\gamma''(t))$ and $\sigma_3 = sd(z_\gamma'''(t))$, then

(1)

$$P(\#\{t \in \tilde{T}_{\text{II}} \cap I_j^{\text{side}}\} = 0) \geq 1 - \exp\left(-\frac{a_j^2 C_{j,\gamma}^2}{2\sigma_2^2}\right).$$

(2)

$$P(\#\{t \in \tilde{T}_{\text{II}} \cap I_j^{\text{mode}}\} = 1) \geq -1 + 2\Phi\left(\frac{|a_j| C_{j,\gamma}}{\sigma_2}\right) - \exp\left(-\frac{a_j^2 D_{j,\gamma}^2}{2\sigma_3^2}\right).$$

(3) For any fixed threshold u , we have

$$\begin{aligned} P(\#\{t \in \tilde{T}_{\text{II}}^+ \cap I_j^{\text{mode}} : y_\gamma'(t) - k(t) > u\} = 1) &\geq 1 - \exp\left(-\frac{a_j^2 D_{j,\gamma}^2}{2\sigma_3^2}\right) - \Phi\left(\frac{u - |a_j| M_{j,\gamma}}{\sigma_1}\right), \\ P(\#\{t \in \tilde{T}_{\text{II}}^- \cap I_j^{\text{mode}} : y_\gamma'(t) - k(t) < -u\} = 1) &\geq 1 - \exp\left(-\frac{a_j^2 D_{j,\gamma}^2}{2\sigma_3^2}\right) + \Phi\left(\frac{u - |a_j| M_{j,\gamma}}{\sigma_1}\right). \end{aligned}$$

Proof. (1). As the probability that there are no local extremum of $y_\gamma'(t)$ in I_j^{side} is greater than the probability that $|y_\gamma''(t)| > 0$ for all $t \in I_j^{\text{side}}$, then

$$\begin{aligned} P(\#\{t \in \tilde{T}_{\text{II}} \cap I_j^{\text{side}}\} = 0) &\geq P(\inf_{I_j^{\text{side}}} |y_\gamma''(t)| > 0) \\ &\geq P(\sup_{I_j^{\text{side}}} |z_\gamma''(t)| < \inf_{I_j^{\text{side}}} |\mu_\gamma''(t)|) \\ &= 1 - P(\sup_{I_j^{\text{side}}} |z_\gamma''(t)| > \inf_{I_j^{\text{side}}} |\mu_\gamma''(t)|) \\ &\geq 1 - \exp\left(-\frac{a_j^2 C_{j,\gamma}^2}{2\sigma_2^2}\right). \end{aligned} \tag{C.45}$$

The last line holds because of Borell-TIS inequality.

(2). The probability that $y'_\gamma(t)$ has no local maximum in I_j^{mode} is less than the probability that $y''_\gamma(v_j - \delta) \leq 0$ or $y''_\gamma(v_j + \delta) \geq 0$. Thus the probability of no local maximum in I_j^{mode} is bounded above by

$$\begin{aligned}
P(\#\{t \in \tilde{T}_\Pi^+ \cap I_j^{\text{mode}}\} = 0) &\leq P(y''_\gamma(v_j - \delta) \leq 0 \cup y''_\gamma(v_j + \delta) \geq 0) \\
&\leq P(y''_\gamma(v_j - \delta) \leq 0) + P(y''_\gamma(v_j + \delta) \geq 0) \\
&= \Phi\left(-\frac{\mu''_\gamma(v_j - \delta)}{\sigma_2}\right) + \Phi\left(\frac{\mu''_\gamma(v_j + \delta)}{\sigma_2}\right) \\
&= 1 - \Phi\left(\frac{\mu''_\gamma(v_j - \delta)}{\sigma_2}\right) + 1 - \Phi\left(-\frac{\mu''_\gamma(v_j + \delta)}{\sigma_2}\right) \\
&\leq 2 - 2\Phi\left(\frac{|a_j|C_{j,\gamma}}{\sigma_2}\right).
\end{aligned}$$

The last line holds because $y''_\gamma(t) \sim N(\mu''_\gamma(t), \sigma_2^2)$, $\mu''_\gamma(v_j - \delta) > |a_j|C_{j,\gamma} > 0$ and $-\mu''_\gamma(v_j + \delta) > |a_j|C_{j,\gamma} > 0$ for $t \in \tilde{T}_\Pi^+ \cap I_j^{\text{mode}}$. Similarly, $P(\#\{t \in \tilde{T}_\Pi^- \cap I_j^{\text{mode}}\} = 0) \leq 2 - 2\Phi\left(\frac{|a_j|C_{j,\gamma}}{\sigma_2}\right)$. Therefore,

$$P(\#\{t \in \tilde{T}_\Pi \cap I_j^{\text{mode}}\} = 0) \leq 2 - 2\Phi\left(\frac{|a_j|C_{j,\gamma}}{\sigma_2}\right).$$

On the other hand, the probability that $y'_\gamma(t)$ has at least two local maxima in I_j^{mode} is less than the probability that $y''_\gamma(t) > 0$ for some $t \in I_j^{\text{mode}}$ and $y''_\gamma(t) < 0$ for some other $t \in I_j^{\text{mode}}$. Thus for $t \in \tilde{T}_\Pi^+ \cap I_j^{\text{mode}}$,

$$\begin{aligned}
P(\#\{t \in \tilde{T}_\Pi^+ \cap I_j^{\text{mode}}\} \geq 2) &\leq P(\sup y''_\gamma(t) > 0 \cap \inf y''_\gamma(t) < 0) \\
&\leq P(\sup y''_\gamma(t) > 0) \wedge P(\inf y''_\gamma(t) < 0) \\
&\leq P(\sup z''_\gamma(t) > \inf -\mu''_\gamma(t)) \wedge P(\sup z''_\gamma(t) > \inf \mu''_\gamma(t)) \\
&\leq \exp\left(-\frac{a_j^2 D_{j,\gamma}^2}{2\sigma_3^2}\right).
\end{aligned}$$

The last line holds because $\mu''_\gamma(t) < 0$ for $t \in \tilde{T}_\Pi^+ \cap I_j^{\text{mode}}$. Similarly, $P(\#\{t \in \tilde{T}_\Pi^- \cap I_j^{\text{mode}}\} \geq 2) \leq \exp\left(-\frac{a_j^2 D_{j,\gamma}^2}{2\sigma_3^2}\right)$. Therefore,

$$P(\#\{t \in \tilde{T}_\Pi \cap I_j^{\text{mode}}\} \geq 2) \leq \exp\left(-\frac{a_j^2 D_{j,\gamma}^2}{2\sigma_3^2}\right).$$

The probability that $y'_\gamma(t)$ has only one local maximum in I_j^{mode} is calculated as

$$\begin{aligned}
&P(\#\{t \in \tilde{T}_\Pi \cap I_j^{\text{mode}}\} = 1) \\
&= 1 - P(\#\{t \in \tilde{T}_\Pi \cap I_j^{\text{mode}}\} = 0) - P(\#\{t \in \tilde{T}_\Pi \cap I_j^{\text{mode}}\} \geq 2) \\
&\geq -1 + 2\Phi\left(\frac{|a_j|C_{j,\gamma}}{\sigma_2}\right) - \exp\left(-\frac{a_j^2 D_{j,\gamma}^2}{2\sigma_3^2}\right).
\end{aligned} \tag{C.46}$$

(3). Since the probability that at least two local maxima of $y'_\gamma(t)$ in I_j^{mode} exceed $u + k(t)$ is less than the probability that $y'_\gamma(t)$ has at least two maxima in I_j^{mode} , then

$$\begin{aligned} & P(\#\{t \in \tilde{T}_{\text{II}}^+ \cap I_j^{\text{mode}} : y'_\gamma(t) - k(t) > u\} \geq 2) \\ & \leq P(\#\{t \in \tilde{T}_{\text{II}}^+ \cap I_j^{\text{mode}}\} \geq 2) \\ & \leq \exp\left(-\frac{a_j^2 D_{j,\gamma}^2}{2\sigma_3^2}\right). \end{aligned}$$

Similarly, $P(\#\{t \in \tilde{T}_{\text{II}}^- \cap I_j^{\text{mode}} : y'_\gamma(t) - k(t) < -u\} \geq 2) \leq \exp\left(-\frac{a_j^2 D_{j,\gamma}^2}{2\sigma_3^2}\right)$.

On the other hand, since the probability that no local maxima of $y'_\gamma(t)$ in I_j^{mode} exceeds $u + k(t)$ is less than the probability that $y'_\gamma(t) - k(t) \leq u$ anywhere in I_j^{mode} , then

$$\begin{aligned} & P(\#\{t \in \tilde{T}_{\text{II}}^+ \cap I_j^{\text{mode}} : y'_\gamma(t) - k(t) > u\} = 0) \\ & \leq P(y'_\gamma(t) - k(t) \leq u \text{ for } \forall t \in I_j^{\text{mode}}) \\ & = P(z'_\gamma(t) + \mu'_\gamma(t) - k(t) \leq u \text{ for } \forall t \in I_j^{\text{mode}}) \\ & \leq \Phi\left(\frac{u - a_j M_{j,\gamma}}{\sigma_1}\right) = \Phi\left(\frac{u - |a_j| M_{j,\gamma}}{\sigma_1}\right). \end{aligned}$$

The last line holds because $a_j > 0$ if $t \in \tilde{T}_{\text{II}}^+ \cap I_j^{\text{mode}}$. Similarly, $P(\#\{t \in \tilde{T}_{\text{II}}^- \cap I_j^{\text{mode}} : y'_\gamma(t) - k(t) < -u\} = 0) \leq \Phi\left(\frac{u - |a_j| M_{j,\gamma}}{\sigma_1}\right)$.

Therefore, the probability that only one local maximum of $y'_\gamma(t)$ in I_j^{mode} exceeds $u + k(t)$ is

$$\begin{aligned} & P(\#\{t \in \tilde{T}_{\text{II}}^+ \cap I_j^{\text{mode}} : y'_\gamma(t) - k(t) > u\} = 1) \\ & = 1 - P(\#\{t \in \tilde{T}_{\text{II}}^+ \cap I_j^{\text{mode}} : y'_\gamma(t) - k(t) > u\} = 0) \\ & \quad - P(\#\{t \in \tilde{T}_{\text{II}}^+ \cap I_j^{\text{mode}} : y'_\gamma(t) - k(t) > u\} \geq 2) \\ & \geq 1 - \Phi\left(\frac{\mu - |a_j| M_{j,\gamma}}{\sigma_1}\right) - \exp\left(-\frac{a_j^2 D_{j,\gamma}^2}{2\sigma_3^2}\right). \end{aligned} \tag{C.47}$$

Similarly, $P(\#\{t \in \tilde{T}_{\text{II}}^- \cap I_j^{\text{mode}} : y'_\gamma(t) - k(t) < -u\} = 1) \geq 1 - \Phi\left(\frac{\mu - |a_j| M_{j,\gamma}}{\sigma_1}\right) - \exp\left(-\frac{a_j^2 D_{j,\gamma}^2}{2\sigma_3^2}\right)$. \square

Lemma S3. Define \mathbb{T}_γ as the transition region, denoted by $\mathbb{T}_\gamma = \mathbb{S}_{1,\gamma} \setminus \mathbb{S}_1 = \cup_{j=1}^J S_{j,\gamma} \setminus S_j$. Let $W_{\text{II},\gamma} = \#\{t \in \tilde{T}_{\text{II}} \cap \mathbb{S}_{1,\gamma}\}$ and $W_{\text{II},\gamma}(u) = \#\{t \in \tilde{T}_{\text{II}}(u) \cap \mathbb{S}_{1,\gamma}\}$, where $W_{\text{II},\gamma}(u) = W_{\text{II},\gamma}^+(u) + W_{\text{II},\gamma}^-(u) = \#\{t \in \tilde{T}_{\text{II}}^+ \cap \mathbb{S}_{1,\gamma}\} + \#\{t \in \tilde{T}_{\text{II}}^- \cap \mathbb{S}_{1,\gamma}\}$. Under the condition (C2), there exist a $\eta > 0$ such that

(1)

$$P(\#\{t \in \tilde{T}_{\text{II}} \cap \mathbb{T}_\gamma\} \geq 1) = o(\exp(-\eta a^2)),$$

(2)

$$P(W_{\text{II},\gamma} = J) = 1 - o(\exp(-\eta a^2)),$$

(3)

$$P(W_{\Pi,\gamma}(u) = J) = 1 - o(\exp(-\eta a^2)),$$

(4)

$$W_{\Pi,\gamma}/L = A + o_p(1),$$

(5)

$$W_{\Pi,\gamma}(u)/W_{\Pi,\gamma} = 1 + o_p(1).$$

Proof. (1). For a $\eta > 0$, as $I_j^{\text{mode}} \subset S_j$ implying $T_{j,\gamma} \subset I_j^{\text{side}}$, then we get

$$\begin{aligned} P(\#\{\tilde{T}_{\Pi} \cap \mathbb{T}_{\gamma} \geq 1\}) &\leq P(\#\{t \in \tilde{T}_{\Pi} \cap (\cup_{j=1}^J I_j^{\text{side}})\} \geq 1) \\ &= P(\cup_{j=1}^J \#\{t \in \tilde{T}_{\Pi} \cap I_j^{\text{side}}\} \geq 1) \\ &\leq \sum_{j=1}^J [1 - P(\#\{t \in \tilde{T}_{\Pi} \cap I_j^{\text{side}}\} = 0)] \\ &\leq \sum_{j=1}^J \exp\left(-\frac{a_j^2 C_{j,\gamma}^2}{2\sigma_2^2}\right) \leq \sum_{j=1}^J \exp\left(-\frac{a^2 C_{\gamma}^2}{2\sigma_2^2}\right) \\ &= \frac{J}{L} L \exp\left(-\frac{a^2 C_{\gamma}^2}{2\sigma_2^2}\right) = o(\exp(-\eta a^2)). \end{aligned}$$

The last line holds because

$$L \exp\left(-\frac{a^2 C_{\gamma}^2}{2\sigma_2^2}\right) = \exp\left\{a^2 \left(\frac{\log L}{a^2} - \frac{C_{\gamma}^2}{2\sigma_2^2}\right)\right\} = o(\exp(-\eta a^2)) \text{ as } \frac{\log L}{a^2} \rightarrow 0.$$

(2).

$$\begin{aligned} P(W_{\Pi,\gamma} = J) &= P(\#\{t \in \tilde{T}_{\Pi} \cap \mathbb{S}_{1,\gamma} = J\}) \\ &\geq P[\cap_{j=1}^J (\#\{t \in \tilde{T}_{\Pi} \cap I_j^{\text{mode}}\} = 1 \cap \#\{t \in \tilde{T}_{\Pi} \cap I_j^{\text{side}}\} = 0)] \\ &\geq 1 - \sum_{j=1}^J [1 - P(\#\{t \in \tilde{T}_{\Pi} \cap I_j^{\text{mode}}\} = 1 \cap \#\{t \in \tilde{T}_{\Pi} \cap I_j^{\text{side}}\} = 0)] \\ &\geq 1 - \sum_{j=1}^J [2 - P(\#\{t \in \tilde{T}_{\Pi} \cap I_j^{\text{mode}}\} = 1) - P(\#\{t \in \tilde{T}_{\Pi} \cap I_j^{\text{side}}\} = 0)] \\ &= 1 - \sum_{j=1}^J [2 - 2\Phi\left(\frac{|a_j| C_{j,\gamma}}{\sigma_2}\right) + \exp\left(-\frac{a_j^2 D_{j,\gamma}^2}{2\sigma_3^2}\right) + \exp\left(-\frac{a_j^2 C_{j,\gamma}^2}{2\sigma_2^2}\right)] \\ &\geq 1 - \frac{J}{L} \left\{2L[1 - \Phi\left(\frac{aC_{\gamma}}{\sigma_2}\right)] + L \exp\left(-\frac{a^2 C_{\gamma}^2}{2\sigma_2^2}\right) + L \exp\left(-\frac{a^2 D_{\gamma}^2}{2\sigma_3^2}\right)\right\} \\ &= 1 - o(\exp(-\eta a^2)). \end{aligned}$$

The last line holds because $L[1 - \Phi(Ka)] \leq L\phi(Ka)/(Ka)$ for any $K > 0$.

(3). Denote by $B_{j,0}$, $B_{j,1}$ and $B_{j,2}$ the events $\#\{t \in \tilde{T}_{\Pi}(u) \cap I_j^{\text{side}}\} = 0$, $\#\{t \in \tilde{T}_{\Pi}^+(u) \cap I_j^{\text{mode}}\} = 1$ and $\#\{t \in \tilde{T}_{\Pi}^-(u) \cap I_j^{\text{mode}}\} = 1$ respectively. Then

$$\begin{aligned}
P(W_{\Pi,\gamma}(u) = J) &= P(W_{\Pi,\gamma}^+ + W_{\Pi,\gamma}^- = J) \geq P(\cap_{j=1}^J (B_{j,0} \cup B_{j,1} \cup B_{j,2})) \\
&\geq 1 - \sum_{j=1}^J [2 - P(B_{j,0}) - P(B_{j,1}) - P(B_{j,2})] \\
&\geq 1 - \sum_{j=1}^J [-1 + 2 \exp(-a_j^2 \frac{D_{j,\gamma}^2}{2\sigma_3^2}) + \exp(-a_j^2 \frac{C_{j,\gamma}^2}{2\sigma_2^2})] \\
&\geq 1 - \sum_{j=1}^J [-1 + 2 \exp(-a^2 \frac{D_{\gamma}^2}{2\sigma_3^2}) + \exp(-a^2 \frac{C_{\gamma}^2}{2\sigma_2^2})] \\
&= 1 - o(\exp(-\eta a^2)).
\end{aligned}$$

(4).

$$\frac{W_{\Pi,\gamma}}{L} = \frac{W_{\Pi,\gamma}}{J} \frac{J}{L} = A(1 + o_p(1)) = A + o_p(1),$$

by the part (2) of this Lemma.

(5). Similar to the proof of part (4), by the part (3), we get $W_{\Pi,\gamma}(u)/L = A + o_p(1)$. Then

$$W_{\Pi,\gamma}(u)/W_{\Pi,\gamma} = (W_{\Pi,\gamma}(u)/L)/(W_{\Pi,\gamma}/L) = 1 + o_p(1).$$

□

D FDR Control and Power Consistency for Type II Change Points

D.1 FDR control

Proof of Theorem 2 (FDR control). Recall that $V_{\Pi}(u) = \#\{t \in \tilde{T}_{\Pi}(u) \cap \mathbb{S}_0\}$ and $W_{\Pi,\gamma}(u) = \#\{t \in \tilde{T}_{\Pi}(u) \cap \mathbb{S}_{1,\gamma}\}$. Let $W_{\Pi}(u) = \#\{t \in \tilde{T}_{\Pi}(u) \cap \mathbb{S}_1\}$ and $V_{\Pi,\gamma}(u) = \#\{t \in \tilde{T}_{\Pi}(u) \cap \mathbb{S}_{0,\gamma}\}$, that is, $V_{\Pi}(u)$ and $W_{\Pi}(u)$ represent the number of local extrema in the *null region* and *signal region* respectively. $V_{\Pi,\gamma}(u)$ and $W_{\Pi,\gamma}(u)$ represent the number of local extrema in the *smoothed null region* and *smoothed signal region* respectively. Note that $R_{\Pi}(u) = \#\{t \in \tilde{T}_{\Pi}(u)\} = V_{\Pi}(u) + W_{\Pi}(u)$. By the definition of FDR for Type II change points detection, for any fixed u , we have

$$\text{FDR}_{\Pi}(u) = E\left[\frac{V_{\Pi}(u)}{V_{\Pi}(u) + W_{\Pi}(u)}\right] = E\left[\frac{V_{\Pi}(u)/L}{V_{\Pi}(u)/L + W_{\Pi}(u)/L}\right]. \quad (\text{D.48})$$

$$\begin{aligned}
P(V_{\Pi,\gamma}(u) = V_{\Pi}(u)) &= 1 - P(V_{\Pi,\gamma}(u) \neq V_{\Pi}(u)) \\
&= 1 - P(\#\{t \in \tilde{T}_{\Pi}(u) \cap \mathbb{T}_{\gamma}\} \geq 1) \\
&\geq 1 - P(\#\{t \in \tilde{T}_{\Pi} \cap \mathbb{T}_{\gamma}\} \geq 1) \\
&= 1 - o(\exp(-\eta a^2)) \rightarrow 1.
\end{aligned}$$

Hence, $V_{\Pi,\gamma}(u) = V_{\Pi}(u) + o_p(1)$. Similarly, we obtain that $W_{\Pi,\gamma}(u) = W_{\Pi}(u) + o_p(1)$.

Then it follows that

$$\begin{aligned}\frac{V_{\Pi}(u)}{L} &= \frac{V_{\Pi}(u)}{V_{\Pi,\gamma}(u)} \frac{V_{\Pi,\gamma}(u)}{L} = [1 + o_p(1)] \frac{[L - J(2c\gamma)]E[\tilde{m}_{z'_\gamma}(U(1), u)]}{L} \\ &= (1 - 2c\gamma A)E[\tilde{m}_{z'_\gamma}(U(1), u)] + o_p(1), \\ \frac{W_{\Pi}(u)}{L} &= \frac{W_{\Pi}(u)}{W_{\Pi,\gamma}(u)} \frac{W_{\Pi,\gamma}(u)}{L} = [1 + o_p(1)][A + o_p(1)] = A + o_p(1).\end{aligned}$$

Hence,

$$\frac{V_{\Pi}(u)/L}{V_{\Pi}(u)/L + W_{\Pi}(u)/L} = \frac{(1 - 2c\gamma A)E[\tilde{m}_{z'_\gamma}(U(1), u)]}{A + (1 - 2c\gamma A)E[\tilde{m}_{z'_\gamma}(U(1), u)]} + o_p(1) < 1.$$

As $\frac{V_{\Pi}(u)}{V_{\Pi}(u) + W_{\Pi}(u)}$ is bounded, by the Dominated Convergence Theorem (DCT),

$$\lim E\left[\frac{V_{\Pi}(u)/L}{V_{\Pi}(u)/L + W_{\Pi}(u)/L}\right] = E\left[\lim \frac{V_{\Pi}(u)/L}{V_{\Pi}(u)/L + W_{\Pi}(u)/L}\right] = \frac{(1 - 2c\gamma A)E[\tilde{m}_{z'_\gamma}(U(1), u)]}{A + (1 - 2c\gamma A)E[\tilde{m}_{z'_\gamma}(U(1), u)]}.$$

That is,

$$\text{FDR}_{\Pi}(u) \rightarrow \frac{(1 - 2c\gamma A)E[\tilde{m}_{z'_\gamma}(U(1), u)]}{A + (1 - 2c\gamma A)E[\tilde{m}_{z'_\gamma}(U(1), u)]}, \quad (\text{D.49})$$

completing the FDR control of part (i) in Theorem 2.

Next we will show the FDR control for random threshold \tilde{u}_{Π} . Let $\tilde{G}(u) = \#\{t \in \tilde{T}_{\Pi}(u)\} / \#\{t \in \tilde{T}_{\Pi}\}$ be the empirical marginal right cdf of $z'_\gamma(t)$ given $t \in \tilde{T}_{\Pi}$. By Benjamini-Hochberg (BH) procedure, the BH threshold \tilde{u}_{Π} satisfies $\alpha\tilde{G}(\tilde{u}_{\Pi}) = k\alpha/m_{\Pi} = F_{z'_\gamma}(\tilde{u}_{\Pi})$, so \tilde{u}_{Π} is the largest u that solves the equation

$$\alpha\tilde{G}(u) = F_{z'_\gamma}(u). \quad (\text{D.50})$$

$$\tilde{G}(u) = \frac{V_{\Pi,\gamma}(u) + W_{\Pi,\gamma}(u)}{V_{\Pi,\gamma} + W_{\Pi,\gamma}} = \frac{V_{\Pi,\gamma}(u)}{V_{\Pi,\gamma}} \frac{V_{\Pi,\gamma}}{V_{\Pi,\gamma} + W_{\Pi,\gamma}} + \frac{W_{\Pi,\gamma}(u)}{W_{\Pi,\gamma}} \frac{W_{\Pi,\gamma}}{V_{\Pi,\gamma} + W_{\Pi,\gamma}},$$

By Lemma 8 in (Schwartzman et al., 2011),

$$\frac{V_{\Pi,\gamma}(u)/L}{V_{\Pi,\gamma}/L} \xrightarrow{P} \frac{E[V_{\Pi,\gamma}(u)]}{E[V_{\Pi,\gamma}]} = F_{z'_\gamma}(u). \quad (\text{D.51})$$

In addition,

$$\frac{V_{\Pi,\gamma}}{V_{\Pi,\gamma} + W_{\Pi,\gamma}} = \frac{V_{\Pi,\gamma}/L}{V_{\Pi,\gamma}/L + W_{\Pi,\gamma}/L} \xrightarrow{P} \frac{E[\tilde{m}_{z'_\gamma}(U(1))](1 - 2c\gamma A)}{E[\tilde{m}_{z'_\gamma}(U(1))](1 - 2c\gamma A) + A},$$

and

$$\frac{W_{\Pi,\gamma}}{V_{\Pi,\gamma} + W_{\Pi,\gamma}} = \frac{W_{\Pi,\gamma}/L}{V_{\Pi,\gamma}/L + W_{\Pi,\gamma}/L} \xrightarrow{P} \frac{A}{E[\tilde{m}_{z'_\gamma}(U(1))](1 - 2c\gamma A) + A}.$$

Combined with (D.50) and part (5) in Lemma S3, we obtain

$$\tilde{G}(u) \xrightarrow{P} F_{z'_\gamma}(u) \frac{E[\tilde{m}_{z'_\gamma}(U(1))](1 - 2c\gamma A)}{E[\tilde{m}_{z'_\gamma}(U(1))](1 - 2c\gamma A) + A} + \frac{A}{E[\tilde{m}_{z'_\gamma}(U(1))](1 - 2c\gamma A) + A}.$$

Plugging $\tilde{G}_1(u)$ by its limit in (D.50) and solving for u gives the deterministic solution

$$F_{z'_\gamma}(u_\Pi^*) = \frac{\alpha A}{A + E[\tilde{m}_{z'_\gamma}(U(1))](1 - 2c\gamma A)(1 - \alpha)}. \quad (\text{D.52})$$

Note that \tilde{u}_Π is the solution of $\alpha\tilde{G}(u) = F_{z'_\gamma}(u)$ and u_Π^* is the solution of $\lim \alpha\tilde{G}(u) = F_{z'_\gamma}(u)$, as $F_{z'_\gamma}^{-1}(\cdot)$ is continuous and monotonic, then we have $\tilde{u}_\Pi \xrightarrow{P} u_\Pi^*$. That is, for any $\epsilon > 0$,

$$P(|\tilde{u}_\Pi - u_\Pi^*| \leq \epsilon) \rightarrow 1.$$

By the definition of FDR, for the random threshold \tilde{u}_Π and any $\epsilon > 0$,

$$\begin{aligned} \text{FDR}_{\Pi, \text{BH}} &= \text{FDR}_\Pi(\tilde{u}_\Pi) = E\left[\frac{V_\Pi(\tilde{u}_\Pi)}{V_\Pi(\tilde{u}_\Pi) + W_\Pi(\tilde{u}_\Pi)}\right] \\ &= E\left[\frac{V_\Pi(\tilde{u}_\Pi)}{V_\Pi(\tilde{u}_\Pi) + W_\Pi(\tilde{u}_\Pi)} \mathbb{1}(|\tilde{u}_\Pi - u_\Pi^*| \leq \epsilon)\right] + E\left[\frac{V_\Pi(\tilde{u}_\Pi)}{V_\Pi(\tilde{u}_\Pi) + W_\Pi(\tilde{u}_\Pi)} \mathbb{1}(|\tilde{u}_\Pi - u_\Pi^*| > \epsilon)\right] \\ &= E\left[\frac{V_\Pi(\tilde{u}_\Pi)}{V_\Pi(\tilde{u}_\Pi) + W_\Pi(\tilde{u}_\Pi)} \mathbb{1}(|\tilde{u}_\Pi - u_\Pi^*| \leq \epsilon)\right] + o(1). \end{aligned}$$

As both $V_\Pi(u)$ and $W_\Pi(u)$ are decreasing with respect to u , then for $\frac{V_\Pi(\tilde{u}_\Pi)}{V_\Pi(\tilde{u}_\Pi) + W_\Pi(\tilde{u}_\Pi)} \mathbb{1}(|\tilde{u}_\Pi - u_\Pi^*| \leq \epsilon)$, it has a lower bound:

$$\frac{V_\Pi(\tilde{u}_\Pi)}{V_\Pi(\tilde{u}_\Pi) + W_\Pi(\tilde{u}_\Pi)} \mathbb{1}(|\tilde{u}_\Pi - u_\Pi^*| \leq \epsilon) \geq \frac{V_\Pi(u_\Pi^* + \epsilon)}{V_\Pi(u_\Pi^* - \epsilon) + W_\Pi(u_\Pi^* - \epsilon)} \mathbb{1}(|\tilde{u}_\Pi - u_\Pi^*| \leq \epsilon),$$

and an upper bound:

$$\frac{V_\Pi(\tilde{u}_\Pi)}{V_\Pi(\tilde{u}_\Pi) + W_\Pi(\tilde{u}_\Pi)} \mathbb{1}(|\tilde{u}_\Pi - u_\Pi^*| \leq \epsilon) \leq \frac{V_\Pi(u_\Pi^* - \epsilon)}{V_\Pi(u_\Pi^* + \epsilon) + W_\Pi(u_\Pi^* + \epsilon)}.$$

Additionally,

$$\begin{aligned} &E\left[\frac{V_\Pi(u_\Pi^* + \epsilon)}{V_\Pi(u_\Pi^* - \epsilon) + W_\Pi(u_\Pi^* - \epsilon)} \mathbb{1}(|\tilde{u}_\Pi - u_\Pi^*| \leq \epsilon)\right] \\ &= E\left[\frac{V_\Pi(u_\Pi^* + \epsilon)}{V_\Pi(u_\Pi^* - \epsilon) + W_\Pi(u_\Pi^* - \epsilon)}\right] P(|\tilde{u}_\Pi - u_\Pi^*| \leq \epsilon) \\ &\rightarrow E\left[\frac{V_\Pi(u_\Pi^* + \epsilon)}{V_\Pi(u_\Pi^* - \epsilon) + W_\Pi(u_\Pi^* - \epsilon)}\right]. \end{aligned}$$

Therefore,

$$\begin{aligned} E\left[\frac{V_\Pi(\tilde{u}_\Pi)}{V_\Pi(\tilde{u}_\Pi) + W_\Pi(\tilde{u}_\Pi)} \mathbb{1}(|\tilde{u}_\Pi - u_\Pi^*| \leq \epsilon)\right] &\geq E\left[\frac{V_\Pi(u_\Pi^* + \epsilon)}{V_\Pi(u_\Pi^* - \epsilon) + W_\Pi(u_\Pi^* - \epsilon)} \mathbb{1}(|\tilde{u}_\Pi - u_\Pi^*| \leq \epsilon)\right], \\ E\left[\frac{V_\Pi(\tilde{u}_\Pi)}{V_\Pi(\tilde{u}_\Pi) + W_\Pi(\tilde{u}_\Pi)} \mathbb{1}(|\tilde{u}_\Pi - u_\Pi^*| \leq \epsilon)\right] &\leq E\left[\frac{V_\Pi(u_\Pi^* - \epsilon)}{V_\Pi(u_\Pi^* + \epsilon) + W_\Pi(u_\Pi^* + \epsilon)}\right], \end{aligned}$$

Since $E[\tilde{m}_{z_\gamma}(U(1), u)]$ is continuous due to Kac-Rice formula, by letting $\epsilon \rightarrow 0$, we have

$$E\left[\frac{V_{\Pi}(\tilde{u}_{\Pi})}{V_{\Pi}(\tilde{u}_{\Pi}) + W_{\Pi}(\tilde{u}_{\Pi})} \mathbb{1}(|\tilde{u}_{\Pi} - u_{\Pi}^*| \leq \epsilon)\right] \rightarrow E\left[\frac{V_{\Pi}(u_{\Pi}^*)}{V_{\Pi}(u_{\Pi}^*) + W_{\Pi}(u_{\Pi}^*)}\right].$$

Therefore,

$$\begin{aligned} \lim \text{FDR}_{\Pi, \text{BH}} &= \lim E\left[\frac{V_{\Pi}(\tilde{u}_{\Pi})}{V_{\Pi}(\tilde{u}_{\Pi}) + W_{\Pi}(\tilde{u}_{\Pi})}\right] \\ &= \lim \left\{ E\left[\frac{V_{\Pi}(\tilde{u}_{\Pi})}{V_{\Pi}(\tilde{u}_{\Pi}) + W_{\Pi}(\tilde{u}_{\Pi})} \mathbb{1}(|\tilde{u}_{\Pi} - u_{\Pi}^*| \leq \epsilon)\right] + o(1) \right\} \\ &= \lim E\left[\frac{V_{\Pi}(u_{\Pi}^*)}{V_{\Pi}(u_{\Pi}^*) + W_{\Pi}(u_{\Pi}^*)}\right] \\ &= E\left[\lim \frac{V_{\Pi}(u_{\Pi}^*)/L}{V_{\Pi}(u_{\Pi}^*)/L + W_{\Pi}(u_{\Pi}^*)/L}\right] \tag{D.53} \\ &= E\left[\frac{F_{z_\gamma}'(u_{\Pi}^*)E[\tilde{m}_{z_\gamma}(U(1))](1 - 2c\gamma A)}{F_{z_\gamma}'(u_{\Pi}^*)E[\tilde{m}_{z_\gamma}(U(1))](1 - 2c\gamma A) + A}\right] \quad (\text{by (D.51)}) \\ &= \alpha \frac{E[\tilde{m}_{z_\gamma}(U(1))](1 - 2c\gamma A)}{E[\tilde{m}_{z_\gamma}(U(1))](1 - 2c\gamma A) + A} \quad (\text{by (D.52)}). \end{aligned}$$

□

D.2 Power consistency

Proof of Theorem 2 (power consistency). By Lemma S2, for any fixed u ,

$$\begin{aligned} \text{Power}_{\Pi, j}(u) &= P(\#\{t \in \tilde{T}_{\Pi}(u) \cap S_j\} \geq 1) \\ &\geq P(\#\{t \in \tilde{T}_{\Pi}(u) \cap I_j^{\text{mode}}\} \geq 1) \\ &\geq 1 - \exp\left(-\frac{a_j^2 D_{j, \gamma}^2}{2\sigma^3}\right) + \Phi\left(\frac{u - |a_j| M_{j, \gamma}}{\sigma_1}\right) \rightarrow 1. \end{aligned}$$

Therefore,

$$\text{Power}_{\Pi}(u) = \frac{1}{J} \sum_{j=1}^J \text{Power}_{\Pi, j}(u) \rightarrow 1.$$

For the random threshold \tilde{u}_{Π} and arbitrary $\epsilon > 0$, we have

$$\begin{aligned} &P(\#\{t \in \tilde{T}_{\Pi}(\tilde{u}_{\Pi}) \cap S_j\} \geq 1) \\ &= P(\#\{t \in \tilde{T}_{\Pi}(\tilde{u}_{\Pi}) \cap S_j\} \geq 1, |\tilde{u}_{\Pi} - u_{\Pi}^*| \leq \epsilon) \\ &\quad + P(\#\{t \in \tilde{T}_{\Pi}(\tilde{u}_{\Pi}) \cap S_j\} \geq 1, |\tilde{u}_{\Pi} - u_{\Pi}^*| > \epsilon). \end{aligned} \tag{D.54}$$

As

$$P(\#\{t \in \tilde{T}_{\Pi}(\tilde{u}_{\Pi}) \cap S_j\} \geq 1, |\tilde{u}_{\Pi} - u_{\Pi}^*| > \epsilon) \leq P(|\tilde{u}_{\Pi} - u_{\Pi}^*| > \epsilon) \rightarrow 0,$$

Then

$$\begin{aligned}
& P(\#\{t \in \tilde{T}_{\text{II}}(\tilde{u}_{\text{II}}) \cap S_j\} \geq 1) \\
& \rightarrow P(\#\{t \in \tilde{T}_{\text{II}}(\tilde{u}_{\text{II}}) \cap S_j\} \geq 1, |\tilde{u}_{\text{II}} - u_{\text{II}}^*| \leq \epsilon) \\
& \geq P(\#\{t \in \tilde{T}_{\text{II}}(u_{\text{II}}^* + \epsilon) \cap S_j\} \geq 1, |\tilde{u}_{\text{II}} - u_{\text{II}}^*| \leq \epsilon) \\
& \geq 1 - P(\#\{t \in \tilde{T}_{\text{II}}(u_{\text{II}}^* + \epsilon) \cap S_j\} = 0) - P(|\tilde{u}_{\text{II}} - u_{\text{II}}^*| > \epsilon) \rightarrow 1.
\end{aligned}$$

The last line holds because for any two events A and B , $P(A \cap B) = 1 - P(A^c \cup B^c) \geq 1 - P(A^c) - P(B^c)$. Therefore,

$$\text{Power}_{\text{II},j}(\tilde{u}_{\text{II}}) \rightarrow 1.$$

And then

$$\text{Power}_{\text{II},\text{BH}} = \text{Power}_{\text{II},\text{BH}}(\tilde{u}_{\text{II}}) = \frac{1}{J} \sum_{j=1}^J \text{Power}_{\text{II},j}(\tilde{u}_{\text{II}}) \rightarrow 1.$$

□

E FDR Control and Power Consistency for Mixture of Type I and Type II Change Points

E.1 FDR control

Proof of Theorem 3 (FDR control). Recall that FDR for mixture of Type I and Type II change points is defined as

$$\text{FDR}_{\text{III}}(u_1, u_2) = E \left\{ \frac{V_{\text{I}\setminus\text{II}}(u_1) + V_{\text{II}}(u_2)}{R_{\text{I}\setminus\text{II}}(u_1) + R_{\text{II}}(u_2)} \right\}.$$

And $\mathbb{S}_{1,\text{I}\setminus\text{II}} = \cup_{j=1}^{J_1} (v_j - b, v_j + b) \setminus \mathbb{S}_{\text{II}}^*$, where v_j is a Type I change point and $\mathbb{S}_{\text{II}}^* = \cup_{i=1}^{R_{\text{II}}} (\hat{v}_i - 2\gamma, \hat{v}_i + 2\gamma)$ for $\hat{v}_i \in \tilde{T}_{\text{II}}$. Let $\mathbb{S}_{1,\gamma,\text{I}\setminus\text{II}}$ and $\mathbb{S}_{0,\gamma,\text{I}\setminus\text{II}}$ be the smoothed signal region and smoothed null region of Type I change points, denoted by $\mathbb{S}_{1,\gamma,\text{I}\setminus\text{II}} = \cup_{j=1}^{J_1} (v_j - c\gamma, v_j + c\gamma) \setminus \mathbb{S}_{\text{II}}^*$ and $\mathbb{S}_{0,\gamma,\text{I}\setminus\text{II}} = U(L) \setminus \mathbb{S}_{1,\gamma,\text{I}\setminus\text{II}}$.

Let $W_{\text{I}\setminus\text{II}}(u_1) = \#\{t \in \tilde{T}_{\text{I}\setminus\text{II}}(u_1) \cap \mathbb{S}_{1,\text{I}\setminus\text{II}}\}$ and $W_{\text{I}\setminus\text{II},\gamma}(u_1) = \#\{t \in \tilde{T}_{\text{I}\setminus\text{II}}(u_1) \cap \mathbb{S}_{1,\gamma,\text{I}\setminus\text{II}}\}$. Then $R_{\text{I}\setminus\text{II}}(u_1) = V_{\text{I}\setminus\text{II}}(u_1) + W_{\text{I}\setminus\text{II}}(u_1)$, and $\text{FDR}_{\text{III}}(u_1, u_2)$ can be rewritten as

$$\begin{aligned}
\text{FDR}_{\text{III}}(u_1, u_2) &= E \left[\frac{V_{\text{I}\setminus\text{II}}(u_1) + V_{\text{II}}(u_2)}{V_{\text{I}\setminus\text{II}}(u_1) + W_{\text{I}\setminus\text{II}}(u_1) + V_{\text{II}}(u_2) + W_{\text{II}}(u_2)} \right] \\
&= E \left\{ E \left[\frac{V_{\text{I}\setminus\text{II}}(u_1) + V_{\text{II}}(u_2)}{V_{\text{I}\setminus\text{II}}(u_1) + W_{\text{I}\setminus\text{II}}(u_1) + V_{\text{II}}(u_2) + W_{\text{II}}(u_2)} \mid V_{\text{II}}(u_2) \right] \right\}
\end{aligned}$$

Let $\Delta(u_2)$ be the length of $\mathbb{S}_{0,\gamma,\text{I}\setminus\text{II}}$, then

$$L - 2c\gamma J_1 - 4\gamma R_{\text{II}}(u_2) \leq \Delta(u_2) \leq L - 2c\gamma J_1.$$

The left inequality holds because some of the falsely detected Type II change points may overlap with Type I change points..

Recall that for the detection of Type II change points in step 1 of Algorithm 3, we have

$$\begin{aligned}\frac{V_{\Pi}(u_2)}{L} &\rightarrow E[\tilde{m}_{z'_\gamma}(U(1), u_2)](1 - 2c\gamma A_2), \\ \frac{W_{\Pi}(u_2)}{L} &\rightarrow A_2.\end{aligned}$$

Since we assume that the distance between neighboring change points are large enough, and the detected Type II change points have been removed when detecting Type I change points, then $V_{I \setminus \Pi}(u_1)$ and $W_{I \setminus \Pi}(u_1)$ only depend on $V_{\Pi}(u_2)$,

$$\begin{aligned}\frac{V_{I \setminus \Pi}(u_1)}{L} | V_{\Pi}(u_2) &\rightarrow E[\tilde{m}_{z''_\gamma}(U(1), u_1)]\Delta(u_2), \\ \frac{W_{I \setminus \Pi}(u_1)}{L} | V_{\Pi}(u_2) &= \frac{W_{I \setminus \Pi}(u_1)}{W_{I \setminus \Pi, \gamma}(u_1)} \frac{W_{I \setminus \Pi, \gamma}(u_1)}{L} = \frac{W_{I \setminus \Pi, \gamma}(u_1)}{L} + o_p(1).\end{aligned}$$

Moreover, notice that the falsely detected Type II change points mainly result from random noise (due to FDR control), which are uniformly distributed over the null signal region of Type I change points. Hence in fact, $\cup_{j=1}^{J_1} (v_j - c\gamma, v_j + c\gamma) \cap \mathbb{S}_{\Pi}^* \approx \emptyset$. Thus $\frac{W_{I \setminus \Pi, \gamma}(u_1)}{L} \rightarrow A_1^* \approx A_1$.

$$\begin{aligned}&\frac{V_{I \setminus \Pi}(u_1) + V_{\Pi}(u_2)}{V_{I \setminus \Pi}(u_1) + W_{I \setminus \Pi}(u_1) + V_{\Pi}(u_2) + W_{\Pi}(u_2)} | V_{\Pi}(u_2) \\ &= \frac{V_{I \setminus \Pi}(u_1)/L + V_{\Pi}(u_2)/L}{V_{I \setminus \Pi}(u_1)/L + W_{I \setminus \Pi}(u_1)/L + V_{\Pi}(u_2)/L + W_{\Pi}(u_2)/L} | V_{\Pi}(u_2) \\ &\rightarrow \frac{E[\tilde{m}_{z''_\gamma}(U(1), u_1)]\Delta(u_2)/L + V_{\Pi}(u_2)/L}{E[\tilde{m}_{z''_\gamma}(U(1), u_1)]\Delta(u_2)/L + V_{\Pi}(u_2)/L + A_1^* + A_2} | V_{\Pi}(u_2).\end{aligned}$$

As $\Delta(u_2) \leq L - 2c\gamma J_1$, by DCT,

$$\begin{aligned}\lim \text{FDR}_{\text{III}}(u_1, u_2) &= \lim E\{E[\frac{V_{I \setminus \Pi}(u_1) + V_{\Pi}(u_2)}{V_{I \setminus \Pi}(u_1) + W_{I \setminus \Pi}(u_1) + V_{\Pi}(u_2) + W_{\Pi}(u_2)} | V_{\Pi}(u_2)]\} \\ &= E\{\lim E[\frac{V_{I \setminus \Pi}(u_1)/L + V_{\Pi}(u_2)/L}{V_{I \setminus \Pi}(u_1)/L + W_{I \setminus \Pi}(u_1)/L + V_{\Pi}(u_2)/L + W_{\Pi}(u_2)/L} | V_{\Pi}(u_2)]\} \quad (\text{E.55}) \\ &\leq \frac{E[\tilde{m}_{z''_\gamma}(U(1), u_1)](1 - 2c\gamma A_1) + E[\tilde{m}_{z'_\gamma}(U(1), u_2)](1 - 2c\gamma A_2)}{E[\tilde{m}_{z''_\gamma}(U(1), u_1)](1 - 2c\gamma A_1) + E[\tilde{m}_{z'_\gamma}(U(1), u_2)](1 - 2c\gamma A_2) + A}.\end{aligned}$$

For the random threshold \tilde{u}_I and \tilde{u}_{Π} ,

$$\begin{aligned}\text{FDR}_{\text{III}}(\tilde{u}_I, \tilde{u}_{\Pi}) &= E[\frac{V_{I \setminus \Pi}(\tilde{u}_I) + V_{\Pi}(\tilde{u}_{\Pi})}{V_{I \setminus \Pi}(\tilde{u}_I) + W_{I \setminus \Pi}(\tilde{u}_I) + V_{\Pi}(\tilde{u}_{\Pi}) + W_{\Pi}(\tilde{u}_{\Pi})}] \\ &= E\{E[\frac{V_{I \setminus \Pi}(\tilde{u}_I) + V_{\Pi}(\tilde{u}_{\Pi})}{V_{I \setminus \Pi}(\tilde{u}_I) + W_{I \setminus \Pi}(\tilde{u}_I) + V_{\Pi}(\tilde{u}_{\Pi}) + W_{\Pi}(\tilde{u}_{\Pi})} | V_{\Pi}(\tilde{u}_{\Pi})]\}.\end{aligned}$$

Similar to (D.53), as $\tilde{u}_I \xrightarrow{P} u_I^*$,

$$\begin{aligned}
& E\left[\frac{V_{I \setminus \Pi}(\tilde{u}_I) + V_{\Pi}(\tilde{u}_{\Pi})}{V_{I \setminus \Pi}(\tilde{u}_I) + W_{I \setminus \Pi}(\tilde{u}_I) + V_{\Pi}(\tilde{u}_{\Pi}) + W_{\Pi}(\tilde{u}_{\Pi})} \middle| V_{\Pi}(\tilde{u}_{\Pi})\right] \\
&= E\left[E\left[\frac{V_{I \setminus \Pi}(\tilde{u}_I) + V_{\Pi}(\tilde{u}_{\Pi})}{V_{I \setminus \Pi}(\tilde{u}_I) + W_{I \setminus \Pi}(\tilde{u}_I) + V_{\Pi}(\tilde{u}_{\Pi}) + W_{\Pi}(\tilde{u}_{\Pi})} \middle| V_{\Pi}(\tilde{u}_{\Pi})\right]\right] \\
&\rightarrow E\left[\frac{V_{\Pi}(\tilde{u}_{\Pi})/L + F_{z_{\gamma}''}(u_I^*)E[\tilde{m}_{z_{\gamma}''}(U(1))]\Delta(\tilde{u}_{\Pi})/L}{V_{\Pi}(\tilde{u}_{\Pi})/L + W_{\Pi}(\tilde{u}_{\Pi})/L + F_{z_{\gamma}''}(u_I^*)E[\tilde{m}_{z_{\gamma}''}(U(1))]\Delta(\tilde{u}_{\Pi})/L + \tilde{A}_1^*}\right],
\end{aligned}$$

where

$$\begin{aligned}
L - 2c\gamma J_1 - 4\gamma R_{\Pi}(\tilde{u}_{\Pi}) &\leq \Delta(\tilde{u}_{\Pi}) \leq L - 2c\gamma J_1, \\
\tilde{A}_1^* &\approx A_1, \\
F_{z_{\gamma}''}(u_I^*) &= \frac{\alpha A_1}{A_1 + (1 - \alpha)E[\tilde{m}_{z_{\gamma}''}(U(1))]\Delta(\tilde{u}_{\Pi})/L}.
\end{aligned}$$

Additionally,

$$\begin{aligned}
F_{z_{\gamma}''}(u_I^*)\Delta(\tilde{u}_{\Pi})/L &= \frac{\alpha A_1 \Delta(\tilde{u}_{\Pi})/L}{A_1 + (1 - \alpha)E[\tilde{m}_{z_{\gamma}''}(U(1))]\Delta(\tilde{u}_{\Pi})/L} \\
&\leq \frac{\alpha A_1 (1 - 2c\gamma A_1)}{A_1 + (1 - \alpha)E[\tilde{m}_{z_{\gamma}''}(U(1))](1 - 2c\gamma A_1)}.
\end{aligned}$$

Therefore,

$$\begin{aligned}
\lim \text{FDR}(\tilde{u}_I, \tilde{u}_{\Pi}) &= \lim E\left\{E\left[\frac{V_{I \setminus \Pi}(\tilde{u}_I) + V_{\Pi}(\tilde{u}_{\Pi})}{V_{I \setminus \Pi}(\tilde{u}_I) + W_{I \setminus \Pi}(\tilde{u}_I) + V_{\Pi}(\tilde{u}_{\Pi}) + W_{\Pi}(\tilde{u}_{\Pi})}\right]\right\} \\
&= E\left[\lim \frac{V_{\Pi}(\tilde{u}_{\Pi})/L + F_{z_{\gamma}''}(u_I^*)E[\tilde{m}_{z_{\gamma}''}(U(1))]\Delta(\tilde{u}_{\Pi})/L}{V_{\Pi}(\tilde{u}_{\Pi})/L + W_{\Pi}(\tilde{u}_{\Pi})/L + F_{z_{\gamma}''}(u_I^*)E[\tilde{m}_{z_{\gamma}''}(U(1))]\Delta(\tilde{u}_{\Pi})/L + \tilde{A}_1^*}\right] \\
&\leq E\left[\lim \frac{V_{\Pi}(\tilde{u}_{\Pi})/L + E[\tilde{m}_{z_{\gamma}''}(U(1))]\frac{\alpha A_1(1 - 2c\gamma A_1)}{A_1 + (1 - \alpha)E[\tilde{m}_{z_{\gamma}''}(U(1))](1 - 2c\gamma A_1)}}{V_{\Pi}(\tilde{u}_{\Pi})/L + W_{\Pi}(\tilde{u}_{\Pi})/L + A_1 + E[\tilde{m}_{z_{\gamma}''}(U(1))]\frac{\alpha A_1(1 - 2c\gamma A_1)}{A_1 + (1 - \alpha)E[\tilde{m}_{z_{\gamma}''}(U(1))](1 - 2c\gamma A_1)}}\right] \\
&= E\left[\frac{V_{\Pi}(u_{\Pi}^*)/L + E[\tilde{m}_{z_{\gamma}''}(U(1))]\frac{\alpha A_1(1 - 2c\gamma A_1)}{A_1 + (1 - \alpha)E[\tilde{m}_{z_{\gamma}''}(U(1))](1 - 2c\gamma A_1)}}{V_{\Pi}(u_{\Pi}^*)/L + A_2 + A_1 + E[\tilde{m}_{z_{\gamma}''}(U(1))]\frac{\alpha A_1(1 - 2c\gamma A_1)}{A_1 + (1 - \alpha)E[\tilde{m}_{z_{\gamma}''}(U(1))](1 - 2c\gamma A_1)}}\right] \\
&\leq \alpha.
\end{aligned}$$

The last line holds because by (D.53)

$$E\left[\frac{V_{\Pi}(u_{\Pi}^*)/L}{V_{\Pi}(u_{\Pi}^*)/L + A_2}\right] \leq \alpha,$$

and on the other hand,

$$\begin{aligned}
& \frac{E[\tilde{m}_{z_{\gamma}''}(U(1))]\frac{\alpha A_1(1 - 2c\gamma A_1)}{A_1 + (1 - \alpha)E[\tilde{m}_{z_{\gamma}''}(U(1))](1 - 2c\gamma A_1)}}{A_1 + E[\tilde{m}_{z_{\gamma}''}(U(1))]\frac{\alpha A_1(1 - 2c\gamma A_1)}{A_1 + (1 - \alpha)E[\tilde{m}_{z_{\gamma}''}(U(1))](1 - 2c\gamma A_1)}} \\
&= \alpha \frac{(1 - 2c\gamma A_1)E[\tilde{m}_{z_{\gamma}''}(U(1))]}{A_1 + (1 - 2c\gamma A_1)E[\tilde{m}_{z_{\gamma}''}(U(1))]} \leq \alpha.
\end{aligned}$$

□

E.2 Power consistency

Proof of Theorem 3 (power consistency). If v_j is a Type II break, then $\text{Power}_{\text{II},j}(u_2) = P(\#\{t \in \tilde{T}_{\text{II}}(u_2) \cap S_j\})$. If v_j is a Type I break, then $\text{Power}_{\text{I},j}(u_1) = P(\#\{t \in \tilde{T}_{\text{I}}(u_1) \cap S_j\})$.

$$\begin{aligned} \text{Power}_{\text{III}}(u_1, u_2) &= \frac{1}{J} \sum_{j=1}^J \left[\text{Power}_{\text{I},j}(u_1) \mathbb{1}(v_j \text{ is Type I}) + \text{Power}_{\text{II},j}(u_2) \mathbb{1}(v_j \text{ is Type II}) \right] \\ &\rightarrow \frac{1}{J} \sum_{j=1}^J [\mathbb{1}(v_j \text{ is Type I}) + \mathbb{1}(v_j \text{ is Type II})] = 1. \end{aligned}$$

Similar to the proof of power consistency of Theorems 1 and 2, for the random threshold \tilde{u}_{I} and \tilde{u}_{II} , if v_j is a Type I break,

$$\text{Power}_{\text{I},j}(\tilde{u}_{\text{I}}) \rightarrow 1,$$

and if v_j is a Type II break,

$$\text{Power}_{\text{II},j}(\tilde{u}_{\text{II}}) \rightarrow 1.$$

Therefore,

$$\text{Power}_{\text{III,BH}} = \text{Power}_{\text{III}}(\tilde{u}_{\text{I}}, \tilde{u}_{\text{II}}) \rightarrow 1.$$

□

References

- D. W. Andrews. Tests for parameter instability and structural change with unknown change point. *Econometrica: Journal of the Econometric Society*, pages 821–856, 1993.
- D. W. Andrews, I. Lee, and W. Ploberger. Optimal changepoint tests for normal linear regression. *Journal of Econometrics*, 70(1):9–38, 1996.
- J. Bai. Least squares estimation of a shift in linear processes. *Journal of Time Series Analysis*, 15(5): 453–472, 1994.
- J. Bai. Estimation of a change point in multiple regression models. *Review of Economics and Statistics*, 79(4):551–563, 1997.
- J. Bai and P. Perron. Estimating and testing linear models with multiple structural changes. *Econometrica*, 66(1):47–78, 1998.
- Y. Bai and A. Safikhani. A unified framework for change point detection in high-dimensional linear models. *arXiv preprint arXiv:2207.09007*, 2022.

- R. Baranowski, Y. Chen, and P. Fryzlewicz. Narrowest-over-threshold detection of multiple change points and change-point-like features. *Journal of the Royal Statistical Society: Series B (Statistical Methodology)*, 81(3):649–672, 2019.
- A. Bulut, A. K. Singh, P. Shin, T. Fountain, H. Jasso, L. Yan, and A. Elgamal. Real-time nondestructive structural health monitoring using support vector machines and wavelets. In *Advanced Sensor Technologies for Nondestructive Evaluation and Structural Health Monitoring*, volume 5770, pages 180–189. SPIE, 2005.
- P.-C. Chang, C.-Y. Fan, and C.-H. Liu. Integrating a piecewise linear representation method and a neural network model for stock trading points prediction. *IEEE Transactions on Systems, Man, and Cybernetics, Part C (Applications and Reviews)*, 39(1):80–92, 2008.
- J. Chen and A. K. Gupta. Parametric statistical change point analysis: with applications to genetics. *Medicine, and Finance*. Springer, 2012.
- D. Cheng and A. Schwartzman. Distribution of the height of local maxima of gaussian random fields. *Extremes*, 18(2):213–240, 2015.
- D. Cheng and A. Schwartzman. Multiple testing of local maxima for detection of peaks in random fields. *The Annals of Statistics*, 45(2):529–556, 2017.
- D. Cheng, Z. He, and A. Schwartzman. Multiple testing of local extrema for detection of change points. *Electronic Journal of Statistics*, 14(2):3705–3729, 2020.
- Y. Ding, X. Yang, A. J. Kavs, and J. Li. A novel piecewise linear segmentation for time series. In *2010 The 2nd International Conference on Computer and Automation Engineering (ICCAE)*, volume 4, pages 52–55. IEEE, 2010.
- K. Frick, A. Munk, and H. Sieling. Multiscale change point inference. *Journal of the Royal Statistical Society: Series B (Statistical Methodology)*, 76(3):495–580, 2014.
- P. Fryzlewicz. Wild binary segmentation for multiple change-point detection. *The Annals of Statistics*, 42(6):2243–2281, 2014.
- P. Fryzlewicz. Narrowest significance pursuit: inference for multiple change-points in linear models. *Journal of the American Statistical Association*, (just-accepted):1–25, 2023.
- C. E. Hann, I. Singh-Levett, B. L. Deam, J. B. Mander, and J. G. Chase. Real-time system identification of a nonlinear four-story steel frame structure—application to structural health monitoring. *IEEE Sensors Journal*, 9(11):1339–1346, 2009.
- N. Hao, Y. S. Niu, and H. Zhang. Multiple change-point detection via a screening and ranking algorithm. *Statistica Sinica*, 23(4):1553, 2013.

- M. Heinonen, H. Mannerström, J. Rousu, S. Kaski, and H. Lähdesmäki. Non-stationary gaussian process regression with hamiltonian monte carlo. In *Artificial Intelligence and Statistics*, pages 732–740. PMLR, 2016.
- P. J. Huber. *Robust statistics*, volume 523. John Wiley & Sons, 2004.
- Y. Hung, Y. Wang, V. Zarnitsyna, C. Zhu, and C. J. Wu. Hidden markov models with applications in cell adhesion experiments. *Journal of the American Statistical Association*, 108(504):1469–1479, 2013.
- S. Hyun, K. Z. Lin, M. G’Sell, and R. J. Tibshirani. Post-selection inference for changepoint detection algorithms with application to copy number variation data. *Biometrics*, 77(3):1037–1049, 2021.
- F. Khan, A. Ghaffar, N. Khan, and S. H. Cho. An overview of signal processing techniques for remote health monitoring using impulse radio uwb transceiver. *Sensors*, 20(9):2479, 2020.
- M. Kharinov. Image segmentation using optimal and hierarchical piecewise-constant approximations. *Pattern recognition and image analysis*, 24(3):409–417, 2014.
- M. Lavielle. Using penalized contrasts for the change-point problem. *Signal processing*, 85(8):1501–1510, 2005.
- H. Li, A. Munk, and H. Sieling. Fdr-control in multiscale change-point segmentation. *Electronic Journal of Statistics*, 10(1):918–959, 2016.
- S. X. Liao and M. Pawlak. On image analysis by moments. *IEEE Transactions on Pattern analysis and machine intelligence*, 18(3):254–266, 1996.
- J. Lu, X. Zheng, Q. Z. Sheng, Z. Hussain, J. Wang, and W. Zhou. Mfe-har: multiscale feature engineering for human activity recognition using wearable sensors. In *Proceedings of the 16th EAI International Conference on Mobile and Ubiquitous Systems: Computing, Networking and Services*, pages 180–189, 2019.
- A. B. Olshen, E. S. Venkatraman, R. Lucito, and M. Wigler. Circular binary segmentation for the analysis of array-based dna copy number data. *Biostatistics*, 5(4):557–572, 2004.
- F. Pein, H. Sieling, and A. Munk. Heterogeneous change point inference. *Journal of the Royal Statistical Society: Series B (Statistical Methodology)*, 79(4):1207–1227, 2017.
- P. Perron. The great crash, the oil price shock, and the unit root hypothesis. *Econometrica: journal of the Econometric Society*, pages 1361–1401, 1989.
- K.-K. Phoon, H. Huang, and S. T. Quek. Simulation of strongly non-gaussian processes using karhunen-loeve expansion. *Probabilistic engineering mechanics*, 20(2):188–198, 2005.

- A. Schwartzman, Y. Gavrilov, and R. J. Adler. Multiple testing of local maxima for detection of peaks in 1d. *Annals of statistics*, 39(6):3290, 2011.
- C. Tebaldi and D. Lobell. Towards probabilistic projections of climate change impacts on global crop yields. *Geophysical Research Letters*, 35(8), 2008.
- A. Tomé and P. Miranda. Piecewise linear fitting and trend changing points of climate parameters. *Geophysical Research Letters*, 31(2), 2004.
- K. Van Laerhoven, E. Berlin, and B. Schiele. Enabling efficient time series analysis for wearable activity data. In *2009 International Conference on Machine Learning and Applications*, pages 392–397. IEEE, 2009.
- L. Y. Vostrikova. Detecting “disorder” in multidimensional random processes. In *Doklady Akademii Nauk*, volume 259, pages 270–274. Russian Academy of Sciences, 1981.
- Y.-C. Yao and S.-T. Au. Least-squares estimation of a step function. *Sankhyā: The Indian Journal of Statistics, Series A*, pages 370–381, 1989.
- M. Yu and E. Ruggieri. Change point analysis of global temperature records. *International Journal of Climatology*, 39(8):3679–3688, 2019.